A Systematic Approach for On-Line Identification of Second-Order Process Model from Relay Feedback Test

Tao Liu and Furong Gao
Dept. of Chemical Engineering, Hong Kong University of Science & Technology, Clear Water Bay, Kowloon, Hong Kong, P.R. China

Youqing Wang
Dept. of Chemical Engineering, Hong Kong University of Science and Technology, Clear Water Bay, Kowloon, Hong Kong, P.R. China
Dept. of Automation, Tsinghua University, Beijing 100084, P.R. China

DOI 10.1002/aic.11476
Published online April 28, 2008 in Wiley InterScience (www.interscience.wiley.com).

Low-order process modeling provides a basis for control system design and on-line autotuning in process control. A systematic on-line identification method is proposed in this article to obtain a second-order-plus-dead-time (SOPDT) model from a single biased/unbiased relay feedback test. The relay response shapes of the three types of SOPDT model, overdamped, critically damped, and underdamped, are first examined and categorized for model structure selection before proceeding with the corresponding parameter identification. Exact expressions of the corresponding limit cycles are derived for assessing process response under relay feedback test. By using the measurable parameters of these limit cycles, the corresponding identification algorithms are subsequently derived in a transparent manner. Two denoising methods are given to cope with measurement noises. Illustrative examples are performed to demonstrate the effectiveness and merits of the proposed identification algorithms. © 2008 American Institute of Chemical Engineers *AIChE J,* 54: 1560–1578, 2008
Keywords: identification, relay feedback test, biased, second-order-plus-dead-time (SOPDT) model, limit cycle, denoising

Introduction

Relay feedback identification has attracted increasing attention in the process community, since the pioneering work of Åström and Hägglund[1] which used relay feedback to generate sustained oscillations of the controlled variable for closed-loop identification. Compared with an open-loop identification such as using a step or impulse excitation signal, the process dynamic response is more effectively excited and it can be better observed with sustained oscillation resulted from a relay feedback test. Furthermore, relay feedback test will not cause the process to drift too far away from its operation level. This is important for many practical cases, in particular for highly nonlinear processes with rigorous operating conditions. Based on the concepts of ultimate gain and ultimate frequency obtained from such experiments, the early

Correspondence concerning this article should be addressed to F. Gao at kefgao@ust.hk.

relay feedback method, autotune variation (ATV),[2] has become a popular identification tool in process industry. Reviews on the rapid development of relay feedback identification for process regulation have recently been addressed by Atherton[3] and Hang et al.[4] Much research effort has been presently devoted to using a single relay feedback test for process identification. There are in general two kinds of relay feedback structure, unbiased (symmetrical) and biased (asymmetrical). On the basis of a single run of unbiased relay feedback test, Vivek and Chidambaram[5] proposed a first-order-plus-dead-time (FOPDT) modeling according to the Fourier analysis of the process response; Panda[6] reported an identification algorithm for obtaining an underdamped second-order-plus-dead-time (SOPDT) model by constructing fitting conditions for the relay response; Huang et al.[7] recently developed an alternative identification method for obtaining FOPDT and underdamped SOPDT models based on the analysis of ultimate frequency. To resolve the difficulty associated with the derivation of the process gain from an unbiased relay feedback test, biased relay feedback identification has been developed.[8,9] Srinivasan and Chidambaram[10] proposed such a FOPDT identification algorithm to effectively represent the process response over the low frequency range. Ramakrishnan and Chidambaram[11] subsequently developed an overdamped SOPDT modeling algorithm to improve the fitting effect of frequency response. Using complex function analysis, Kaya and Atherton[12] proposed a so-called A-locus identification algorithm for obtaining a FOPDT or overdamped SOPDT model from a single biased relay feedback test.

It has been widely recognized that the dynamics of most chemical processes can be well represented by a low-order process model, e.g., FOPDT or SOPDT, for the practical purposes of control system design and on-line autotuning.[13] The choice of a suitable model structure is a fundamental step for identification. By categorizing the relay response shapes for a variety of processes, Thyagarajan and Yu[14] suggested to use three model structures for relay feedback identification, FOPDT, critically damped SOPDT, and higher order model with repetitive poles. By comparison, Panda and Yu[15] claimed that FOPDT, critically damped and underdamped SOPDT models could work well for depicting different process response characteristics under relay feedback test. Luyben[16] discussed the efficiency of obtaining a FOPDT model from an unbiased relay feedback test. Recent papers[17,18] demonstrated that a FOPDT model can represent the frequency response characteristic of low- or high-order processes with desirable accuracy over the phase range of $(-\pi, 0)$.

In view of that a SOPDT model can give better fitting than a FOPDT model for a real high-order process, and the three types of SOPDT model, overdamped, critically damped, and underdamped, can be effectively used to represent the dynamic response characteristics for a wide variety of chemical processes, a systematic on-line identification method is proposed in this article to obtain such a SOPDT model from a single biased/unbiased relay feedback test. The guidelines for model structure selection are established by classifying the relay response shapes from a large number of relay identification tests on these SOPDT models with different parameter settings. The relay response expressions of these models

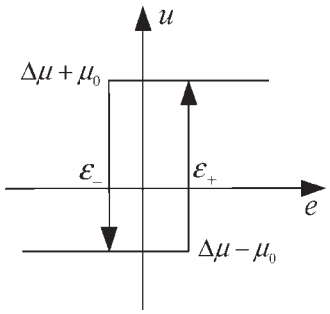

Figure 1. Relay function.

are then derived analytically for assessing process response under relay feedback test. For each model structure, two identification algorithms are respectively given according to whether a biased or an unbiased relay test is used. Two denoising methods are presented to guarantee identification robustness against measurement noises.

On-line relay feedback implementation

To procure the process dynamic response information for process regulation and on-line autotuning, it is often desired to perform identification test around the process operation level. That is to say, nonzero initial conditions are required for on-line relay feedback test. A biased relay function, depicted in Figure 1, may be in practice specified as

$$u(t) = \begin{cases} u_+ & \text{for } \{e(t) > \varepsilon_+\} \text{ or } \{e(t) \geq \varepsilon_- \text{ and } u(t_-) = u_+\} \\ u_- & \text{for } \{e(t) < \varepsilon_-\} \text{ or } \{e(t) \leq \varepsilon_+ \text{ and } u(t_-) = u_-\} \end{cases}$$

where $u_+ = \Delta\mu + \mu_0$ and $u_- = \Delta\mu - \mu_0$ denote, respectively, the positive and negative relay magnitudes; ε_+ and ε_- denote, respectively, the positive and negative switch hysteresis. Note that letting $\Delta\mu = 0$ and $|\varepsilon_+| = |\varepsilon_-|$ leads to an unbiased relay function.

An on-line relay feedback test may be constructed as shown in Figure 2, where r is the process set-point, y the process output, and u_- the relay output. The initial output of the relay is assumed as u for zero input, as set in many existing commercial instruments. The setting of u_+ and u_- should be based on the admissible fluctuation range of the process output around its operational level. It is evident that a larger magnitude of the relay output will facilitate the observation in more details of the process dynamic response. To avoid measurement noises causing incorrect relay switches, the hysteresis for relay switch should be introduced in practice. It is suggested that the magnitudes of ε_+ and ε_- should be set at least twice over the noise band, together with an upper limit almost equal to 0.95 times of the absolute minimum of u_+ and u_-.[19] After the process reaches its operational level, a short "listening period" (e.g., 20–100 samples) may be adopted for reference to set ε_+ and ε_- properly.

A scenario of on-line relay feedback response is shown in Figure 3a, where the process output response and the relay output are put together for illustration. It can be seen that the relay feedback test begins at $t = 20$(s) while the process set-point is taken as $r = 5$. Then, the process output response moves into steady oscillation after several relay switches. For

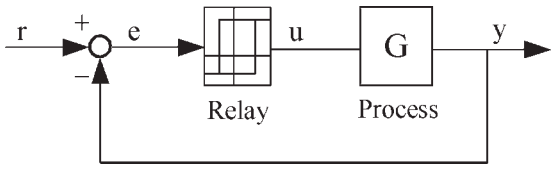

Figure 2. Block diagram of relay feedback test.

the convenience of analysis, we may shift the initial relay response of the process output to the origin in the referential coordinates as shown in Figure 3b, where A_+ denotes the positive amplitude in a steady oscillation period (i.e., limit cycle), and A_- the negative amplitude. The steady oscillation period can be computed as $P_u = P_+ + P_-$, where P_+ denotes the half period corresponding to the relay output u_+ and P_- the other half period corresponding to u_-. Thus, by decomposing the process dynamic response from the set-point value, the resulting limit cycle can be separately studied to derive the process model for dynamic response. Before proceeding with the corresponding identification algorithms, it is preferred to have a discussion on model structure selection for properly representing a real process response under relay feedback test.

Classification of relay response shapes

Overdamped, critically damped, and underdamped SOPDT models differ from each other in the relay response shapes. Given the relay response shape of a real process, it is desirable to find a suitable model structure, such that the best response fitting can be acquired. For reference, Table 1 shows the relay responses of the three types of SOPDT model with different parameter settings under a biased relay test. All of the model gains have been taken as the unity for benchmark comparison.

From the relay response shapes shown in Table 1, the guidelines for model structure selection can be drawn as the following:

(1) Given the same damping ratio (ζ), SOPDT models with the similar ratio of θ/τ have the similar relay response shapes;

(2) For an overdamped ($\xi > 1$) SOPDT model, the relay response shape is similar to a triangular waveform with sharp edges and peaks;

(3) For underdamped ($\xi < 1$) and critically damped ($\xi = 1$) SOPDT models, the relay response shapes are similar to a sinusoidal waveform with smooth curvature and rounded peak, and such characteristics become more apparent as ξ becomes smaller. When $\theta/\tau \gg 1$, the relay response shape of a critically damped SOPDT model tends to be a rectangular waveform following the relay output shape;

(4) For critically damped and overdamped SOPDT models, the relay responses move into a limit cycle almost after a single period of the relay output. The first relay response period is very close (or even the same) in magnitude and shape to the following periods;

(5) For an underdamped SOPDT model, as ξ becomes smaller, more periods of the relay output are required for the relay response to move into a limit cycle, and multiple peaks are likely to occur in the limit cycle when $\theta/\tau \gg 1$;

(6) For the three types of SOPDT model, the amplitude of limit cycle is proportional to the ratio of θ/τ with a fixed ξ, and inversely proportional to ξ with a fixed ratio of θ/τ.

With the above guidelines, a suitable model structure can be intuitively chosen by comparing the relay response shape of a real process with the referential relay shapes of Table 1. Note that the use of biased or unbiased relay test and the height of the relay do not change the relay response shape. A reasonable estimate of ξ and the ratio of θ/τ can also be obtained according to the referential model parameter settings of Table 1. Subsequently, parameter identification for the suitable model structure may be proceeded to refine the identification accuracy.

It should be noted that the above guidelines facilitates reducing computation effort. To assemble an automatic procedure for model identification, the fitting criterion of the maximal frequency response error (ERR) or the step response error (*err*), as will be detailed in the later part, may be used to automatically determine the most suitable model structure, that is to say, the algorithms to be developed respectively for the three types of SOPDT model, overdamped, critically damped, and underdamped, may be simultaneously used to obtain three models according to the experimental data of relay test, and then choose the most suitable one that results in the minimum of the fitting criterion.

Relay response expressions and identification algorithms

To assess the fluctuation range of process output around its set-point under relay feedback test, the relay response of the process model may be used for reference. The exact relay response expressions of the three types of SOPDT model are respectively derived as follows, together with the corresponding identification algorithms. Both biased and unbiased relay tests are considered.

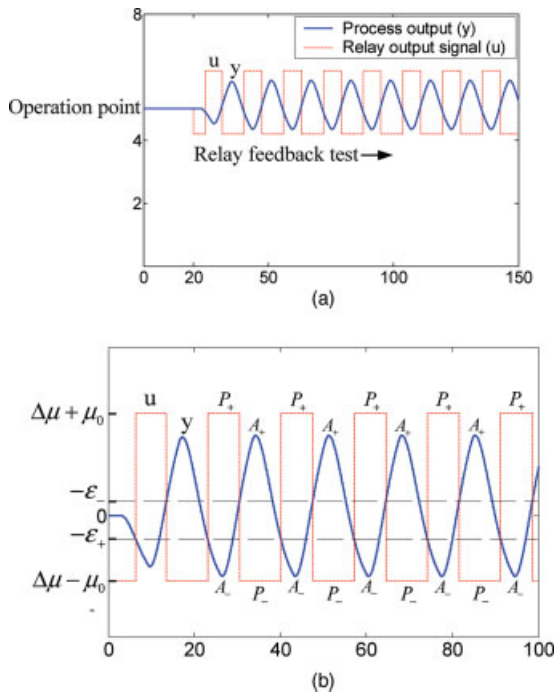

Figure 3. On-line relay feedback response (a) and the shifted version for analysis (b).

[Color figure can be viewed in the online issue, which is available at www.interscience.wiley.com.]

Table 1. Relay Response Shapes of SOPDT Processes with Different Parameter Values. [Color figure can be viewed in the online issue, which is available at www.interscience.wiley.com.]

	$\xi = 0.2$	$\xi = 0.5$	$\xi = 1.0$	$\xi = 5.0$
$\theta = 0.1$ $\tau = 0.1$	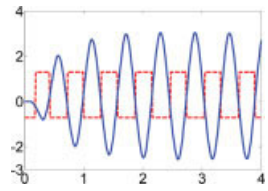	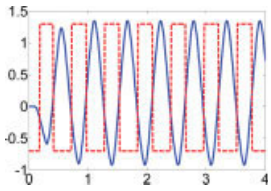	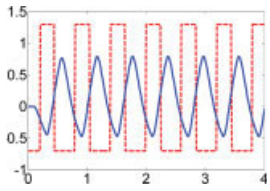	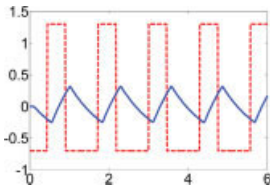
$\theta = 0.1$ $\tau = 1.0$	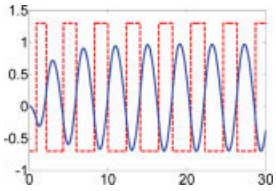	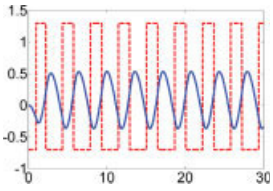	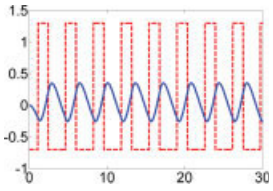	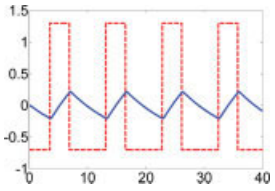
$\theta = 0.1$ $\tau = 10$	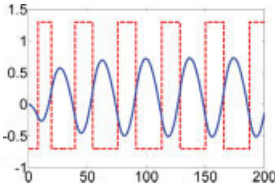	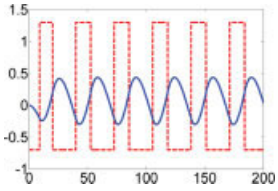	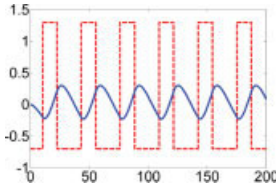	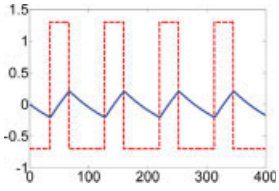
$\theta = 1.0$ $\tau = 0.1$	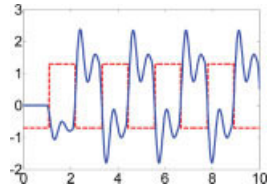	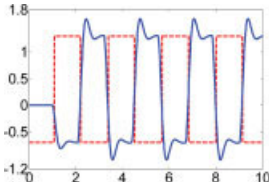	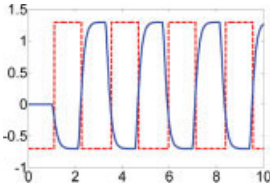	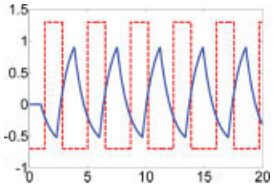
$\theta = 1.0$ $\tau = 1.0$	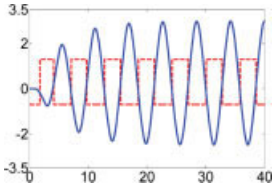	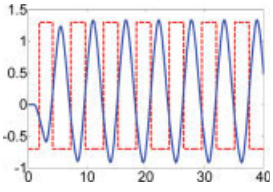	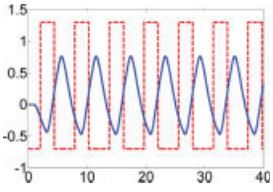	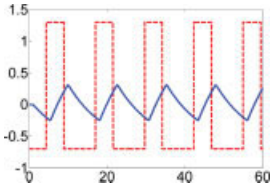
$\theta = 1.0$ $\tau = 10$	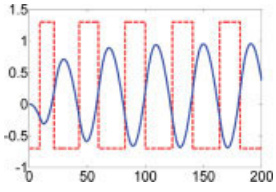	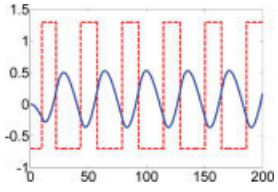	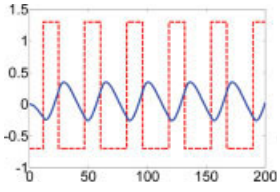	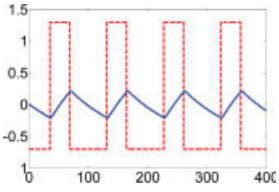
$\theta = 10$ $\tau = 1.0$	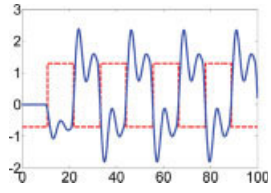	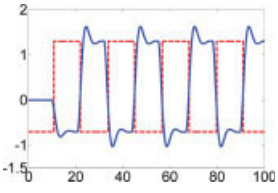	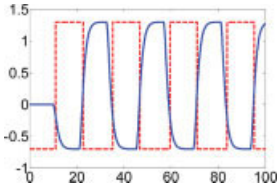	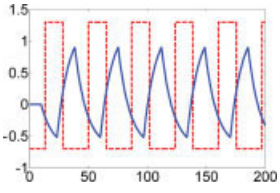
$\theta = 10$ $\tau = 10$	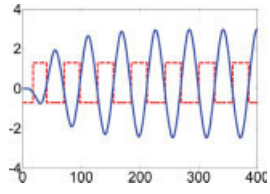	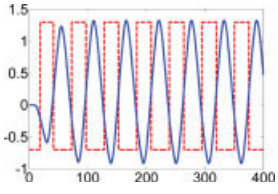	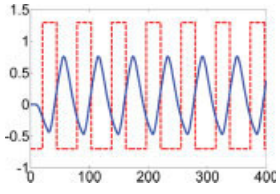	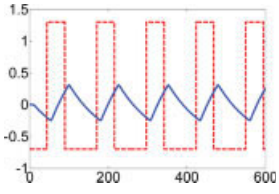

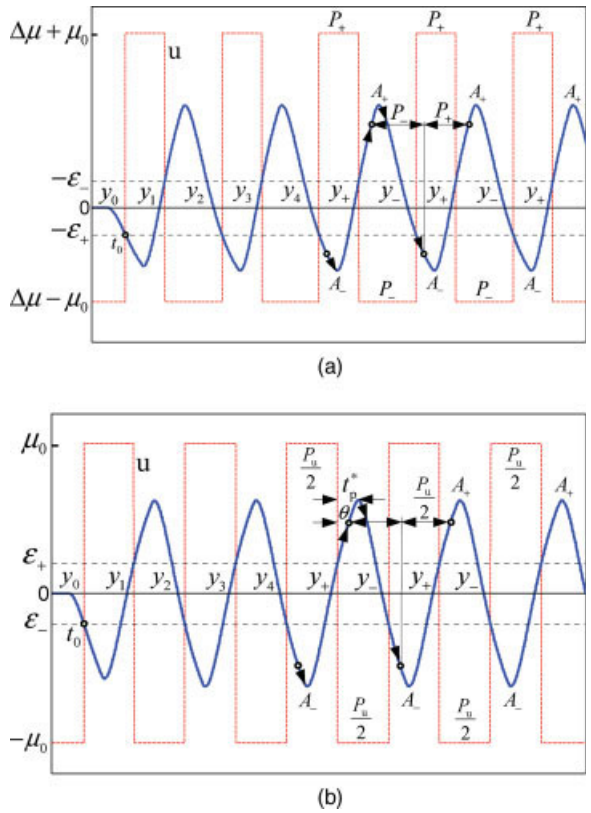

Figure 4. Limit cycle analysis for critically damped SOPDT.

[Color figure can be viewed in the online issue, which is available at www.interscience.wiley.com.]

Critically-damped SOPDT model

A critically damped second-order process is usually described in the form of

$$G_C = \frac{k_p e^{-\theta s}}{(\tau_p s + 1)^2} \tag{1.1}$$

The following proposition gives the exact relay response expression for steady oscillation.

Proposition 1. *For a critically damped second-order process modeled by (1.1) under a biased relay test as shown in Figure 4a, the resulting limit cycle of the process output response is characterized by*

$$y_+(t) = k_p(\Delta\mu + \mu_0) - 2k_p\mu_0 e^{-\frac{t}{\tau_p}}\left(E_1 + \frac{E_1 t + E_2}{\tau_p}\right), \quad t \in [0, P_+] \tag{1.2}$$

$$y_-(t) = k_p(\Delta\mu - \mu_0) - 2k_p\mu_0 e^{-\frac{t}{\tau_p}}\left(F_1 + \frac{F_1 t + F_2}{\tau_p}\right), \quad t \in (P_+, P_u] \tag{1.3}$$

where $y_+(t)$ *is for* $t \in [0, P_+]$ *while* $y_-(t)$ *is for* $t \in (P_+, P_u]$, $E_2 < 0 < E_1$, $F_1 < 0 < F_2$ *and*

$$E_1 = \frac{1 - e^{-\frac{p_-}{\tau_p}}}{1 - e^{-\frac{p_u}{\tau_p}}} \tag{1.4}$$

$$E_2 = \frac{p_u e^{-\frac{p_u}{\tau_p}}(1 - e^{-\frac{p_-}{\tau_p}})}{(1 - e^{-\frac{p_u}{\tau_p}})^2} - \frac{p_- e^{-\frac{p_-}{\tau_p}}}{1 - e^{-\frac{p_u}{\tau_p}}} \tag{1.5}$$

$$F_1 = -\frac{1 - e^{-\frac{p_+}{\tau_p}}}{1 - e^{-\frac{p_u}{\tau_p}}} \tag{1.6}$$

$$F_2 = -\frac{p_u e^{-\frac{p_u}{\tau_p}}(1 - e^{-\frac{p_+}{\tau_p}})}{(1 - e^{-\frac{p_u}{\tau_p}})^2} + \frac{p_+ e^{-\frac{p_+}{\tau_p}}}{1 - e^{-\frac{p_u}{\tau_p}}} \tag{1.7}$$

Proof. See Appendix (I). □

If an unbiased relay feedback test is used as shown in Figure 4b, then $\Delta\mu = 0$ and $P_+ = P_- = P_u/2$. By substituting them into (1.2–1.7), we can obtain the corresponding expression,

$$y_+(t) = -y_-(t) = k_p\mu_0 - 2k_p\mu_0 e^{-\frac{t}{\tau_p}}\left(E_1 + \frac{E_1 t + E_2}{\tau_p}\right) \tag{1.8}$$

where $y_+(t)$ is for $t \in [0, P_u/2]$, $y_-(t)$ for $t \in (P_u/2, P_u]$, and

$$E_1 = \frac{1}{1 + e^{-\frac{p_u}{2\tau_p}}} \tag{1.9}$$

$$E_2 = -\frac{p_u e^{-\frac{p_u}{2\tau_p}}}{2(1 + e^{-\frac{p_u}{2\tau_p}})^2} \tag{1.10}$$

Note that in the limit cycle, the process output is a periodic function with respect to the oscillation angular frequency, $\omega_u = 2\pi/P_u$. By using the idea of time shift, we may view it as a periodic signal from the very beginning, so its Fourier transform can be derived as

$$Y(j\omega_u) = \lim_{N\to\infty} N \int_0^{P_u} y_{os}(t) e^{-j\omega_u t} dt = \lim_{N\to\infty} N \int_{t_{os}}^{t_{os}+P_u} y(t) e^{-j\omega_u t} dt \tag{1.11}$$

where $y_{os}(t) = y(t)$ for $t \in [t_{os}, \infty)$ and t_{os} may be taken as any relay switch point in steady oscillation, such that the influence from the initial process response to the above periodic integral can be excluded.

Similarly, it follows that

$$U(j\omega_u) = \lim_{N\to\infty} N \int_{t_{os}}^{t_{os}+P_u} u(t) e^{-j\omega_u t} dt \tag{1.12}$$

Thereby, the process frequency response at ω_u can be obtained as

$$G(j\omega_u) = \frac{Y(j\omega_u)}{U(j\omega_u)} = \frac{\int_{t_{os}}^{t_{os}+P_u} y(t) e^{-j\omega_u t} dt}{\int_{t_{os}}^{t_{os}+P_u} u(t) e^{-j\omega_u t} dt} = A_u e^{j\varphi_u} \tag{1.13}$$

The numerical integral in (1.13) may be computed using the trapezoidal rule or the fast Fourier transform (FFT) for $Y(j\omega_u)$ and $U(j\omega_u)$.

It should be noted that $\angle G(j\omega_u) = -\pi$ had been used for parameter identification in the existing literature[1,2,7–9,20,21] based on the describing function analysis. Such exercise may result in degraded identification accuracy since $\angle G(j\omega_u)$ is

actually larger than $-\pi$ due to the phase lag caused by the relay, as illustrated by the later examples.

In the case that a biased relay test is used, the process gain can be derived from (1.13) as

$$k_p = G(0) = \frac{\int_{t_{os}}^{t_{os}+P_u} y(t)dt}{\int_{t_{os}}^{t_{os}+P_u} u(t)dt} \tag{1.14}$$

It can be derived from (1.2) and (1.3) that

$$\frac{dy_+(t)}{dt} = \frac{2k_p\mu_0(E_1t+E_2)}{\tau_p^2}e^{-\frac{t}{\tau_p}} \tag{1.15}$$

$$\frac{dy_-(t)}{dt} = \frac{2k_p\mu_0(F_1t+F_2)}{\tau_p^2}e^{-\frac{t}{\tau_p}} \tag{1.16}$$

Thereby, it can be concluded that $y_+(t)$ does not increase monotonously for $t \in [0, P_+]$, and correspondingly, $y_-(t)$ does not decrease monotonously for $t \in (P_+, P_u]$.

By substituting the process model in (1.1) into the frequency response fitting condition shown in (1.13), the process time constant can be derived as

$$\tau_p = \frac{1}{\omega_u}\sqrt{\frac{k_p}{A_u} - 1} \tag{1.17}$$

Using the phase fitting condition,

$$-\theta\omega_u - 2\arctan(\tau_p\omega_u) = \varphi_u, \quad \varphi_u \in (-\pi, -\pi/2), \tag{1.18}$$

the process time delay can be derived as

$$\theta = -\frac{1}{\omega_u}[\varphi_u + 2\arctan(\tau_p\omega_u)] \tag{1.19}$$

Hence, the algorithm for identification of a critically damped SOPDT model from a biased relay test can be summarized in the following algorithm named Algorithm-C-A:

(i) Measure P_+ and P_- from the limit cycle;
(ii) Compute $G(j\omega_u)$ from (1.13);
(iii) Compute the process gain, k_p, from (1.14);
(iv) Compute the process time constant, τ_p, from (1.17);
(v) Compute the process time delay, θ, from (1.19).

In the case that an unbiased relay test is used, by letting (1.15) equal zero we can compute the time to reach the peak value of $y_+(t)$ (or $y_-(t)$) as

$$t_p = -\frac{E_2}{E_1} = \frac{p_u}{2(1+e^{\frac{p_u}{2\tau_p}})} \tag{1.20}$$

In fact, the time to reach the process output peak from the initial relay switch point in a half period of the relay, t_p^*, can be measured as shown in Figure 4b. It follows that

$$t_p = t_p^* - \theta \tag{1.21}$$

Substituting (1.19) and (1.20) into (1.21) yields

$$t_p^* + \frac{1}{\omega_u}[\varphi_u + 2\arctan(\tau_p\omega_u)] = \frac{p_u}{2(1+e^{\frac{p_u}{2\tau_p}})} \tag{1.22}$$

It can be seen that both the left- and right-hand sides of (1.22) increase monotonously with respect to τ_p. For $\tau_p \in (0, \infty)$, the left-hand side takes a value in the range of $(t_p^* + \varphi_u/\omega_u, t_p^* + (\pi + \varphi_u)/\omega_u)$ while the right-hand side is in the range of $(0, p_u/4)$. Hence, there exists only finite solutions of τ_p for (1.22), which can be derived using any iterative algorithm such as the Newton-Raphson method. The initial estimation of τ_p for iteration may be taken as $\widehat{\tau}_p = P_u/2 - t_p^*$, in view of that the influence of the process time constant to the relay response corresponds to this time interval.

The process time delay can then be derived from (1.19), and the process gain can be inversely derived from the magnitude fitting condition as indicated in (1.17), i.e.,

$$k_p = A_u(\tau_p^2\omega_u^2 + 1) \tag{1.23}$$

Therefore, the algorithm for identification of a critically damped SOPDT model from an unbiased relay test can be summarized in the following algorithm named Algorithm-C-B:

(i) Measure P_+, P_-, and t_p^* from the limit cycle;
(ii) Compute $G(j\omega_u)$ from (1.13);
(iii) Compute the process time constant, τ_p, from (1.22) using the Newton-Raphson iteration method. The initial estimation of τ_p for iteration may be taken as $\widehat{\tau}_p = P_u/2 - t_p^*$.
(iv) Compute the process time delay, θ, from (1.19).
(v) Compute the process gain, k_p, from (1.23).
(vi) End the algorithm if the fitting constraint of relay response, $\sum_{k=1}^{N}[\widehat{y}(kT_s + t_{os}) - y(kT_s + t_{os})]^2/N < \varepsilon$, is satisfied, where $\widehat{y}(kT_s + t_{os})$ and $y(kT_s + t_{os})$ denotes respectively the model and process responses in the limit cycle, T_s is the sampling period with $N = P_u/T_s$, and ε is a user-specified fitting threshold that may be set between $0.01\% \sim 1\%$. Otherwise, change the initial estimation of τ_p and go to step (iii).

Note that for critically damped second-order processes with dominant time delay ($\theta/\tau \gg 1$), $y_+(t)$ increases monotonously while $y_-(t)$ decreases monotonously owing to $E_2 \to 0$ and $F_2 \to 0$. Accordingly, the process time delay can be directly obtained as the time to reach the positive peak (A_+) of the process output response from the initial relay switch point in a negative half period of the relay, so that the process time constant and gain can then be respectively derived from (1.19) and (1.23) for simplicity.

Overdamped SOPDT model

An overdamped second-order process is usually described in the form of

$$G_O = \frac{k_p e^{-\theta s}}{(\tau_1 s + 1)(\tau_2 s + 1)} \tag{2.1}$$

where $\tau_1 > \tau_2 > 0$ is assumed without loss of generality. The following proposition gives the exact relay response expression for steady oscillation.

Proposition 2. *For an overdamped second-order process modeled by (2.1) under a biased relay test as shown in Figure 5a, the resulting limit cycle of the process output response is characterized by*

$$y_+(t) = k_p(\Delta\mu + \mu_0) - 2k_p\mu_0\left(\frac{\tau_1E_1}{\tau_1 - \tau_2}e^{-\frac{t}{\tau_1}} - \frac{\tau_2E_2}{\tau_1 - \tau_2}e^{-\frac{t}{\tau_2}}\right), \quad t \in [0, P_+] \tag{2.2}$$

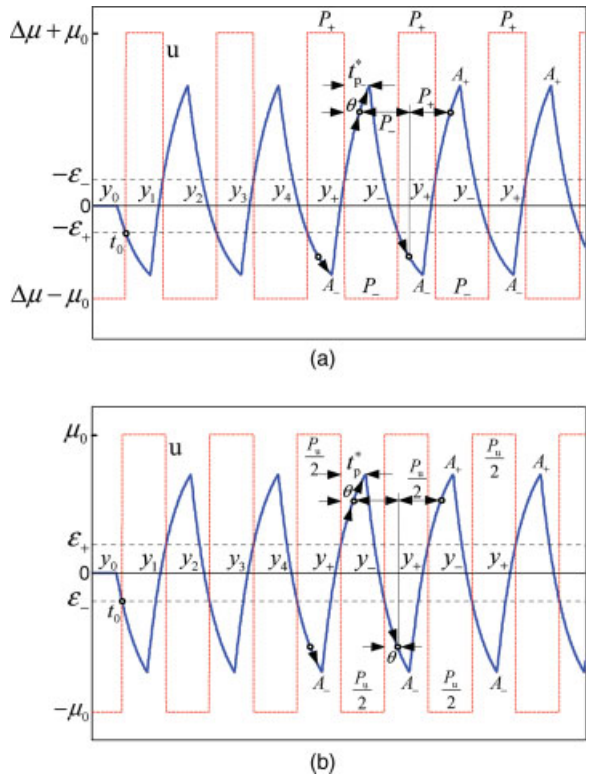

Figure 5. Limit cycle analysis for overdamped SOPDT.

[Color figure can be viewed in the online issue, which is available at www.interscience.wiley.com.]

$$y_-(t) = k_p(\Delta\mu - \mu_0) - 2k_p\mu_0\left(\frac{\tau_1 F_1}{\tau_1 - \tau_2}e^{-\frac{t}{\tau_1}} - \frac{\tau_2 F_2}{\tau_1 - \tau_2}e^{-\frac{t}{\tau_2}}\right), \quad t \in [P_+, P_u] \tag{2.3}$$

where $0 < E_1 < E_2, F_2 < F_1 < 0$, *and*

$$E_1 = \frac{1 - e^{-\frac{p_-}{\tau_1}}}{1 - e^{-\frac{p_u}{\tau_1}}} \tag{2.4}$$

$$E_2 = \frac{1 - e^{-\frac{p_-}{\tau_2}}}{1 - e^{-\frac{p_u}{\tau_2}}} \tag{2.5}$$

$$F_1 = -\frac{1 - e^{-\frac{p_+}{\tau_1}}}{1 - e^{-\frac{p_u}{\tau_1}}} \tag{2.6}$$

$$F_2 = -\frac{1 - e^{-\frac{p_+}{\tau_2}}}{1 - e^{-\frac{p_u}{\tau_2}}} \tag{2.7}$$

Proof. See Appendix (II). □

If an unbiased relay test is used as shown in Figure 5b, by substituting $\Delta\mu = 0$ and $P_+ = P_- = P_u/2$ into (2.2–2.7) we obtain the corresponding expression,

$$y_+(t) = -y_-(t) = k_p\mu_0 - 2k_p\mu_0\left(\frac{\tau_1 E_1}{\tau_1 - \tau_2}e^{-\frac{t}{\tau_1}} - \frac{\tau_2 E_2}{\tau_1 - \tau_2}e^{-\frac{t}{\tau_2}}\right) \tag{2.8}$$

where

$$E_1 = \frac{1}{1 + e^{-\frac{p_u}{2\tau_1}}} \tag{2.9}$$

$$E_2 = \frac{1}{1 + e^{-\frac{p_u}{2\tau_2}}} \tag{2.10}$$

In the case that a biased relay test is used, the process gain can be derived from (1.14). Substituting (2.1) into the frequency response fitting condition shown in (1.13), we can obtain

$$\frac{k_p}{\sqrt{(\tau_1^2\omega_u^2 + 1)(\tau_2^2\omega_u^2 + 1)}} = A_u \tag{2.11}$$

$$-\theta\omega_u - \arctan(\tau_1\omega_u) - \arctan(\tau_2\omega_u) = \varphi_u, \quad \varphi_u \in (-\pi, -\pi/2) \tag{2.12}$$

By letting $\frac{dy_-(t)}{dt} = 0$, the time to reach the single extreme value of $y_-(t)$ can be derived as

$$t_{p_-} = \frac{\tau_1\tau_2}{\tau_1 - \tau_2}\ln\frac{F_2}{F_1} \tag{2.13}$$

Note that the time to reach the single extreme value of $y_-(t)$ from the initial relay switch point in a negative half period of the relay, $t^*_{p_-}$, can be measured as shown in Figure 5a. It follows that

$$t_{p_-} = t^*_{p_-} - \theta \tag{2.14}$$

Substituting (2.11–2.13) into (2.14) to eliminate τ_2 and θ yields

$$\frac{\tau_1\tau_2}{\tau_1 - \tau_2}\ln\frac{F_2}{F_1} = t^*_{p_-} + \frac{1}{\omega_u}[\varphi_u + \arctan(\tau_1\omega_u) + \arctan(\tau_2\omega_u)] \tag{2.15}$$

where

$$\tau_2 = \frac{1}{\omega_u}\sqrt{\frac{k_p^2}{A_u^2(\tau_1^2\omega_u^2 + 1)} - 1} \tag{2.16}$$

Thereby, (2.15) becomes a transcendental equation with respect to τ_1. We can solve this equation with the Newton-Raphson method. The initial estimation of τ_1 for iteration may be taken as

$$\widehat{\tau}_1 = \frac{1}{\omega_u}\sqrt{\frac{k_p}{A_u} - 1} \tag{2.17}$$

which may be derived from (2.11) by letting $\tau_1 = \tau_2$.

The other process time constant and the time delay can then be derived from (2.16) and (2.12).

Hence, the algorithm for identification of an overdamped SOPDT model from a biased relay test can be summarized in the following algorithm named Algorithm-O-A:

(i) Measure P_+, P_-, and $t^*_{p_-}$ from the limit cycle;
(ii) Compute $G(j\omega_u)$ using (1.13);
(iii) Compute the process gain, k_p, from (1.14);
(iv) Compute the process time constant, τ_1, from (2.15) using the Newton-Raphson iteration method. The initial estimation of τ_1 for iteration may be taken from (2.17);
(v) Compute the process time constant, τ_2, from (2.16);
(vi) Compute the process time delay, θ, from (2.12);
(vii) End the algorithm if the fitting constraint of relay response, $\sum_{k=1}^{N}[\widehat{y}(kT_s + t_{os}) - y(kT_s + t_{os})]^2/N < \varepsilon$, is satis-

fied. Otherwise, change the initial estimation of τ_1 and go to step (iv).

In the case that an unbiased relay test is used, it follows from (2.8) that there exist two boundary conditions

$$y_+\left(\frac{P_u}{2}-\theta\right)=k_p\mu_0-2k_p\mu_0 \times\left(\frac{\tau_1E_1}{\tau_1-\tau_2}e^{-\frac{P_u-2\theta}{2\tau_1}}-\frac{\tau_2E_2}{\tau_1-\tau_2}e^{-\frac{P_u-2\theta}{2\tau_2}}\right)=\varepsilon_+ \quad (2.18)$$

$$y_+(t_p)=k_p\mu_0-2k_p\mu_0\left(\frac{\tau_1E_1}{\tau_1-\tau_2}e^{-\frac{t_p}{\tau_1}}-\frac{\tau_2E_2}{\tau_1-\tau_2}e^{-\frac{t_p}{\tau_2}}\right)=A_- \quad (2.19)$$

where t_p is the time to reach the single extreme value of $y_+(t)$ (or $y_-(t)$) which can be derived from $\frac{dy_+(t)}{dt}=0$ as

$$t_p=\frac{\tau_1\tau_2}{\tau_1-\tau_2}\ln\frac{E_2}{E_1} \quad (2.20)$$

Note that

$$t_p=t_p^*-\theta \quad (2.21)$$

where t_p^* is the time to reach the single extreme value of $y_+(t)$ (or $y_-(t)$) from the initial relay switch point in a half period of the relay, which can be measured from the limit cycle.

It follows from dividing (2.18) by (2.19) that

$$\varepsilon_+\left(1-\frac{2\tau_1E_1}{\tau_1-\tau_2}e^{-\frac{t_p}{\tau_1}}+\frac{2\tau_2E_2}{\tau_1-\tau_2}e^{-\frac{t_p}{\tau_2}}\right) =A_-\left(1-\frac{2\tau_1E_1}{\tau_1-\tau_2}e^{-\frac{P_u-2\theta}{2\tau_1}}+\frac{2\tau_2E_2}{\tau_1-\tau_2}e^{-\frac{P_u-2\theta}{2\tau_2}}\right) \quad (2.22)$$

Using the frequency response fitting condition shown in (2.11) and (2.12), we can obtain

$$k_p=A_u\sqrt{(\tau_1^2\omega_u^2+1)(\tau_2^2\omega_u^2+1)} \quad (2.23)$$

$$\theta=-\frac{1}{\omega_u}[\varphi_u+\arctan(\tau_1\omega_u)+\arctan(\tau_2\omega_u)] \quad (2.24)$$

Substituting (2.20) and (2.24) into (2.21) yields an implicit equation with respect to τ_1 and τ_2,

$$F_1(\tau_1,\tau_2)=0 \quad (2.25)$$

Likewise, substituting (2.20) and (2.24) into (2.22) yields another implicit equation with respect to τ_1 and τ_2,

$$F_2(\tau_1,\tau_2)=0 \quad (2.26)$$

Therefore, we can solve (2.25) and (2.26) together to find the solution pair of τ_1 and τ_2. This can be performed by using a nonlinear programming algorithm. The initial values of τ_1 and τ_2 for iteration may be roughly estimated from the referential relay response shapes of Table 1. The search direction may be chosen as the gradients of $F_1(\tau_1, \tau_2)$ and $F_2(\tau_1, \tau_2)$. Thus, the iteration procedure can be programmed using a first-order Taylor expansion as

$$F_1(\tau_{1,k+1},\tau_{2,k+1})=F_1(\tau_{1,k},\tau_{2,k})+\left.\frac{\partial F_1}{\partial\tau_1}\right|_{\tau_{i,k}}\cdot\Delta\tau_1+\left.\frac{\partial F_1}{\partial\tau_2}\right|_{\tau_{i,k}}\cdot\Delta\tau_2 \quad (2.27)$$

$$F_2(\tau_{1,k+1},\tau_{2,k+1})=F_2(\tau_{1,k},\tau_{2,k})+\left.\frac{\partial F_2}{\partial\tau_1}\right|_{\tau_{i,k}}\cdot\Delta\tau_1+\left.\frac{\partial F_2}{\partial\tau_2}\right|_{\tau_{i,k}}\cdot\Delta\tau_2 \quad (2.28)$$

where $F_i(\tau_{1,k}, \tau_{2,k})$ denotes the value of $F_i(\tau_1, \tau_2)$ at the kth iteration step for $i = 1, 2.$, while $\left.\frac{\partial F_1}{\partial\tau_i}\right|_{\tau_{i,k}}$ is the partial derivative of F_i (τ_1, τ_2) with respect to τ_i at the kth step for $i = 1, 2.$ $\Delta\tau_i (i = 1, 2.)$ are the search steps which may be practically selected as 0.01 to guarantee the achievable accuracy. The optimal objective function for convergence can be specified as

$$J_{\min}=\sqrt{\frac{1}{2}[F_1^2(\tau_{1,k+1}),(\tau_{2,k+1})+F_2^2(\tau_{1,k+1}),(\tau_{2,k+1})]}<\delta \quad (2.29)$$

where δ is the convergent threshold which may be set between $0.1\% \sim 1\%$. To avoid unexpected local optimal solutions for τ_1 and τ_2, the aforementioned fitting constraint of relay response can be utilized to screen out the suitable solution pair.

The process gain and time delay can then be derived from (2.23) and (2.24), respectively.

Hence, the algorithm for identification of an overdamped SOPDT model from an unbiased relay test can be summarized in the following algorithm named Algorithm-O-B:

(i) Measure A_+(or A_-), P_u and t_p^* from the limit cycle;

(ii) Compute $G(j\omega_u)$ using (1.13).

(iii) Compute the process time constants, τ_1 and τ_2, from (2.25) and (2.26) using the nonlinear programming algorithm given in (2.27–2.29). The initial values of τ_1 and τ_2 for iteration may be estimated from the referential relay response shapes of Table 1.

(iv) Compute the process gain, k_p, using (2.23);

(v) Compute the process time delay, θ, from (2.24);

(vi) End the algorithm if the fitting constraint of relay response, $\sum_{k=1}^{N}[\hat{y}(kT_s+t_{os})-y(kT_s+t_{os})]^2/N<\varepsilon$, is satisfied. Otherwise, change the initial estimation of τ_1 and τ_2 and go to step (iii).

It should be noted that for overdamped second-order processes with dominant time delay ($\theta/\tau_1 \gg 1$ and $\theta/\tau_2 \gg 1$), $y_+(t)$ increases monotonously while $y_-(t)$ decreases monotonously owing to $E_1 \approx E_2 \approx 1$ and $F_1 \approx F_2 \approx -1$. Therefore, the process time delay can be directly obtained as the time to reach the positive peak (A_+) of the process output response from the initial relay switch point in a negative half period of the relay. The process time constants τ_1 and τ_2 can then be derived by solving (2.22) and (2.24) together.

Underdamped SOPDT model

An underdamped second-order process is usually described in the form of

$$G_U=\frac{k_pe^{-\theta s}}{\tau_p^2s^2+2\xi\tau_ps+1} \quad (3.1)$$

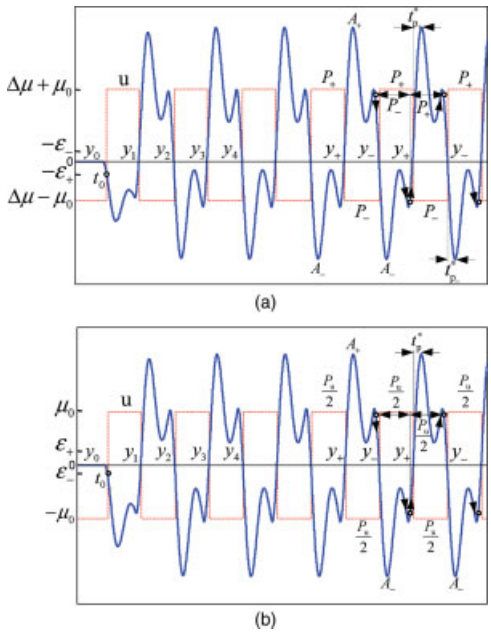

Figure 6. Limit cycle analysis for underdamped SOPDT.

[Color figure can be viewed in the online issue, which is available at www.interscience.wiley.com.]

where $\xi \in (0, 1)$ is customarily named as the process damping ratio, and τ_p is a time constant equal to the reciprocal of ω_p (named as the natural frequency). The following proposition gives the exact relay response expression for steady oscillation.

Proposition 3. *For an underdamped second-order process modeled by (3.1) under a biased relay test as shown in Figure 6a, the resulting limit cycle of the process output response is characterized by*

$$y_+(t) = k_p(\Delta\mu + \mu_0) - \frac{2k_p\mu_0\rho_1}{\eta\gamma} e^{-\frac{\xi t}{\tau_p}} \sin\left(\frac{\eta t}{\tau_p} + \psi_1\right), \quad t \in [0, P_+] \tag{3.2}$$

$$y_-(t) = k_p(\Delta\mu - \mu_0) + \frac{2k_p\mu_0\rho_2}{\eta\gamma} e^{-\frac{\xi t}{\tau_p}} \sin\left(\frac{\eta t}{\tau_p} + \psi_2\right), \quad t \in (P_+, P_u] \tag{3.3}$$

where $\eta = \sqrt{1-\xi^2}$, $\rho_1 = \sqrt{U_1^2 + V_1^2}$, $\rho_2 = \sqrt{U_2^2 + V_2^2}$, $\psi_1 = \tan^{-1}(V_1/U_1)$, $\psi_2 = \tan^{-1}(V_2/U_2)$, $\phi = \tan^{-1}(\sqrt{1-\xi^2}/\xi)$, and

$$\gamma = 1 - 2e^{-\frac{P_u\xi}{\tau_p}} \cos\frac{\eta P_u}{\tau_p} + e^{-\frac{2P_u\xi}{\tau_p}} \tag{3.4}$$

$$U_1 = \cos\phi - e^{-\frac{P_u\xi}{\tau_p}} \cos\left(\phi - \frac{\eta P_u}{\tau_p}\right) - e^{-\frac{P_-\xi}{\tau_p}}\left[\cos\left(\phi + \frac{\eta P_-}{\tau_p}\right) - e^{-\frac{P_u\xi}{\tau_p}} \cos\left(\phi - \frac{\eta P_+}{\tau_p}\right)\right] \tag{3.5}$$

$$V_1 = \sin\phi - e^{-\frac{P_u\xi}{\tau_p}} \sin\left(\phi - \frac{\eta P_u}{\tau_p}\right) - e^{-\frac{P_-\xi}{\tau_p}}\left[\sin\left(\phi + \frac{\eta P_-}{\tau_p}\right) - e^{-\frac{P_u\xi}{\tau_p}} \sin\left(\phi - \frac{\eta P_+}{\tau_p}\right)\right] \tag{3.6}$$

$$U_2 = \cos\phi - e^{-\frac{P_u\xi}{\tau_p}} \cos\left(\phi - \frac{\eta P_u}{\tau_p}\right) - e^{-\frac{P_+\xi}{\tau_p}}\left[\cos\left(\phi + \frac{\eta P_+}{\tau_p}\right) - e^{-\frac{P_u\xi}{\tau_p}} \cos\left(\phi - \frac{\eta P_-}{\tau_p}\right)\right] \tag{3.7}$$

$$V_2 = \sin\phi - e^{-\frac{P_u\xi}{\tau_p}} \sin\left(\phi - \frac{\eta P_u}{\tau_p}\right) - e^{-\frac{P_+\xi}{\tau_p}}\left[\sin\left(\phi + \frac{\eta P_+}{\tau_p}\right) - e^{-\frac{P_u\xi}{\tau_p}} \sin\left(\phi - \frac{\eta P_-}{\tau_p}\right)\right] \tag{3.8}$$

Proof. See Appendix (III). □

If an unbiased relay feedback test is used as shown in Figure 6b, by substituting $\Delta\mu = 0$ and $P_+ = P_- = P_u/2$ into (3.2–3.7) we obtain the corresponding expression,

$$y_+(t) = -y_-(t) = k_p\mu_0 - \frac{2k_p\mu_0\rho}{\eta\gamma} e^{-\frac{\xi t}{\tau_p}} \sin\left(\frac{\eta t}{\tau_p} + \psi\right) \tag{3.9}$$

where $\rho = \sqrt{U^2 + V^2}$, $\psi = \tan^{-1}(V/U)$, and

$$U = \cos\phi - e^{-\frac{P_u\xi}{\tau_p}} \cos\left(\phi - \frac{\eta P_u}{\tau_p}\right) - e^{-\frac{P_u\xi}{2\tau_p}}\left[\cos\left(\phi + \frac{\eta P_u}{2\tau_p}\right) - e^{-\frac{P_u\xi}{\tau_p}} \cos\left(\phi - \frac{\eta P_u}{2\tau_p}\right)\right] \tag{3.10}$$

$$V = \sin\phi - e^{-\frac{P_u\xi}{\tau_p}} \sin\left(\phi - \frac{\eta P_u}{\tau_p}\right) - e^{-\frac{P_u\xi}{2\tau_p}}\left[\sin\left(\phi + \frac{\eta P_u}{2\tau_p}\right) - e^{-\frac{P_u\xi}{\tau_p}} \sin\left(\phi - \frac{\eta P_u}{2\tau_p}\right)\right] \tag{3.11}$$

It can be verified by using (3.9–3.11) that the relay response expression for an underdamped SOPDT process reported in the recent paper[22] is inaccurate, and then was misused in the sequential papers.[6,15]

In the case that a biased relay test is used, the process gain can be derived from (1.14). By using the frequency response fitting condition shown in (1.13), we can obtain

$$\frac{k_p}{\sqrt{(1-\tau_p^2\omega_u^2)^2 + 4\xi^2\tau_p^2\omega_u^2}} = A_u \tag{3.12}$$

$$-\theta\omega_u - \arctan\left(\frac{2\xi\tau_p\omega_u}{1-\tau_p^2\omega_u^2}\right) = \varphi_u, \quad \varphi_u \in (-\pi, -\pi/2) \tag{3.13}$$

It follows from (3.12) that

$$\tau_p = \begin{cases} \dfrac{1}{\omega_u}\sqrt{1 - 2\xi^2 + \sqrt{\dfrac{k_p^2}{A_u^2} + 4\xi^2(\xi^2-1)}} & \text{or} \\ \dfrac{1}{\omega_u}\sqrt{1 - 2\xi^2 + \sqrt{\dfrac{k_p^2}{A_u^2} + 4\xi^2(\xi^2-1)}}, & 0 < \xi < \sqrt{2}/2; \\ \dfrac{1}{\omega_u}\sqrt{1 - 2\xi^2 - \sqrt{\dfrac{k_p^2}{A_u^2} + 4\xi^2(\xi^2-1)}}, & \xi \geq \sqrt{2}/2; \end{cases} \tag{3.14}$$

$$\theta = -\frac{1}{\omega_u}\left[\varphi_u + \arctan\left(\frac{2\xi\tau_p\omega_u}{1-\tau_p^2\omega_u^2}\right)\right] \tag{3.15}$$

It can be derived from (3.2) and (3.3) that

$$\frac{dy_+(t)}{dt} = -\frac{2k_p\mu_0\rho_1}{\eta\gamma\tau_p}e^{-\frac{\xi t}{\tau_p}}\left[\eta\cos\left(\frac{\eta t}{\tau_p}+\psi_1\right) - \xi\sin\left(\frac{\eta t}{\tau_p}+\psi_1\right)\right] \tag{3.16}$$

$$\frac{dy_-(t)}{dt} = \frac{2k_p\mu_0\rho_2}{\eta\gamma\tau_p}e^{-\frac{\xi t}{\tau_p}}\left[\eta\cos\left(\frac{\eta t}{\tau_p}+\psi_2\right) - \xi\sin\left(\frac{\eta t}{\tau_p}+\psi_2\right)\right] \tag{3.17}$$

Then, by letting $\frac{dy_+(t)}{dt} = 0$ and $\frac{dy_-(t)}{dt} = 0$, the time to reach the peak(s) of $y_+(t)$ and $y_-(t)$ can be obtained as

$$t_{p_+,k} = \frac{\tau_p}{\eta}(\phi - \psi_1 + k\pi), \quad k = 0,\ 1,\ 2, \ldots. \tag{3.18}$$

$$t_{p_-,k} = \frac{\tau_p}{\eta}(\phi - \psi_2 + k\pi), \quad k = 0,\ 1,\ 2, \ldots. \tag{3.19}$$

In fact, if there exist several peaks of $y_+(t)$ (or $y_-(t)$) as shown in Figure 6a, the time to reach the largest peak denoted as A_+ (or A_-) from the terminal relay switch point in the corresponding half period of the relay, t^*_{p+} (or t^*_{p-}), can be easily measured. It follows that

$$\begin{aligned} t_{p_+,k} - t_{p_-,k} = \frac{\tau_p}{\eta}(\psi_2 - \psi_1) &= P_+ - \theta + t^*_{p_+} - (P_- - \theta + t^*_{p_-}) \\ &= P_+ - P_- + t^*_{p_+} - t^*_{p_-} \end{aligned} \tag{3.20}$$

It can be seen from (3.20) that $t_{p+,k} - t_{p-,k}$ takes the same value as long as the corresponding peaks of $y_+(t)$ and $y_-(t)$ are measured for computation.

Substituting (3.14) into (3.20) to eliminate τ_p yields a transcendental equation with respect to ξ. We can solve this equation with the Newton-Raphson method. The initial value of ξ for iteration may be roughly estimated from the referential relay response shapes of Table 1. Note that the physical constraint, $0 < \xi < 1$, can be used to limit the search region and directly exclude those unsuitable solutions.

Accordingly, the process time constant and time delay can then be derived from (3.14) and (3.15), respectively. Note that when $0 < \xi < \sqrt{2}/2$, we can exclude the excessive solution of τ_p as shown in (3.14) by means of the iterative algorithm for ξ. To relieve the computation effort, it is suggested to first use the search step, $\xi = 0.01$, to locate θ and τ_p with a loose fitting constraint of the relay response, and then to rectify the search step as $\xi = 0.001$ in conjunction with a much tighter fitting threshold for better identification accuracy.

Therefore, the algorithm for identification of an underdamped SOPDT model from a biased relay test can be summarized in the following algorithm named Algorithm-U-A:

(i) Measure P_+, P_-, t^*_{p+}, and t^*_{p-} from the limit cycle;

(ii) Compute $G(j\omega_u)$ using (1.13);

(iii) Compute the process gain, k_p, using (1.14);

(iv) Compute the process damping ratio, ξ, from the equation resulting from substituting (3.14) into (3.20) by using the Newton-Raphson iteration method. The initial value of ξ for iteration may be estimated from the referential relay response shapes of Table 1;

(v) Compute the process time constant, τ_p, from (3.14);

(vi) Compute the process time delay, θ, from (3.15);

(vii) End the algorithm if the fitting constraint of relay response, $\sum_{k=1}^{N}[\widehat{y}(kT_s + t_{os}) - y(kT_s + t_{os})]^2/N < \varepsilon$, is satisfied. Otherwise, change the initial estimation of ξ and go to step (iv).

It should be noted that though we can obtain from (3.12) that

$$\xi = \frac{1}{2\tau_p\omega_u}\sqrt{\frac{k_p^2}{A_u^2} - (1-\tau_p^2\omega_u^2)^2} \tag{3.21}$$

and then numerically solve τ_p from a transcendental equation resulting from substituting (3.21) into (3.20), the computation effort may be much larger than that for solving ξ, because the initial estimation of τ_p is more difficult and so is for its possible range. Hence, it is not recommended unless a rough value of τ_p can be known a priori in practice.

In the case that an unbiased relay test is used, it follows from (3.9) that

$$\begin{aligned} y_+\left(\frac{P_u}{2} - \theta\right) &= k_p\mu_0 - \frac{2k_p\mu_0\rho}{\eta\gamma}e^{-\frac{\xi(P_u-2\theta)}{2\tau_p}}\sin\left(\frac{\eta(P_u-2\theta)}{2\tau_p}+\psi\right) \\ &= \varepsilon_+ \end{aligned} \tag{3.22}$$

$$y_+(t_p) = k_p\mu_0 - \frac{2k_p\mu_0\rho}{\eta\gamma}e^{-\frac{\xi t_p}{\tau_p}}\sin\left(\frac{\eta t_p}{\tau_p}+\psi\right) = A_+ \tag{3.23}$$

where t_p is the time to reach the largest peak of $y_+(t)$ if there exist several peaks as shown in Figure 6b, which can be derived from $\frac{dy_+(t)}{dt} = 0$ as

$$t_p = \frac{\tau_p}{\eta}(\phi - \psi + k\pi) \tag{3.24}$$

where k can be determined by using the physical constraint

$$t_p = \frac{P_u}{2} - \theta + t^*_p \tag{3.25}$$

where t^*_p is the time to reach the largest peak of $y_+(t)$ (or $y_-(t)$) from the terminal relay switch point in the corresponding half period of the relay; That is, k should be taken to satisfy

$$t^*_p < t_p < \frac{P_u}{2} + t^*_p \tag{3.26}$$

It follows from dividing (3.22) from (3.23) that

$$\begin{aligned} &\varepsilon_+\left[1 - \frac{2\rho}{\eta\gamma}e^{-\frac{\xi t_p}{\tau_p}}\sin\left(\frac{\eta t_p}{\tau_p}+\psi\right)\right] \\ &\quad = A_+\left[1 - \frac{2\rho}{\eta\gamma}e^{-\frac{\xi(P_u-2\theta)}{2\tau_p}}\sin\left(\frac{\eta(P_u-2\theta)}{2\tau_p}+\psi\right)\right] \end{aligned} \tag{3.27}$$

By using the frequency response fitting condition shown in (3.12) and (3.13), we can obtain

$$k_p = A_u\sqrt{(1-\tau_p^2\omega_u^2)^2 + 4\xi^2\tau_p^2\omega_u^2} \tag{3.28}$$

$$\theta = -\frac{1}{\omega_u}\left[\varphi_u + \arctan\left(\frac{2\xi\tau_p\omega_u}{1-\tau_p^2\omega_u^2}\right)\right] \tag{3.29}$$

Substituting (3.24) and (3.29) into (3.25) to eliminate t_p and θ yields an implicit equation with respect to τ_p and ξ,

$$H_1(\tau_p, \xi) = 0 \tag{3.30}$$

Likewise, substituting (3.24) and (3.29) into (3.27) to eliminate t_p and θ yields another implicit equation with respect to τ_p and ξ,

$$H_2(\tau_p, \xi) = 0 \tag{3.31}$$

Therefore, we can solve (3.30) and (3.31) together to find the solution pair of τ_p and ξ. This can be performed by using a nonlinear programming as that for Algorithm-O-B. The initial values of τ_p and ξ for iteration may be estimated from the referential relay response shapes of Table 1, and the physical constraint $0 < \xi < 1$ can be used to limit the search region and directly exclude those unsuitable solution pairs.

The process gain and time delay can then be derived from (3.28) and (3.29), respectively.

Hence, the algorithm for identification of an underdamped SOPDT model from an unbiased relay test can be summarized in the following algorithm named Algorithm-U-B:

(i) Measure A_+ (or A_-), P_u and t_p^* from the limit cycle;

(ii) Compute $G(j\omega_u)$ using (1.13);

(iii) Compute the process time constant, τ_p, and damping ratio, ξ, from (3.30) and (3.31) by using a nonlinear programming as in Algorithm-O-B. The initial values of τ_p and ξ for iteration may be estimated from the referential relay response shapes of Table 1;

(iv) Compute the process gain, k_p, from (3.28);

(v) Compute the process time delay, θ, from (3.29);

(vi) End the algorithm if the fitting constraint of relay response, $\sum_{k=1}^{N}[\hat{y}(kT_s + t_{os}) - y(kT_s + t_{os})]^2/N < \varepsilon$, is satisfied. Otherwise, change the initial estimation of τ_p and ξ and go to step (iii).

Measurement noise issue

Measurement noise is usually unavoidable in engineering practice. In the context of process identification, noise-to-signal ratio (NSR) is generally evaluated as

$$\mathrm{NSR} = \frac{\mathrm{mean}(\mathrm{abs}(\mathrm{noise}))}{\mathrm{mean}(\mathrm{abs}(\mathrm{signal}))} \tag{4.1}$$

To reduce the influence from measurement noises, it is suggested that when a biased relay feedback test is performed, the measured values of P_+, P_-, A_+, and A_- for $10 \sim 20$ periods in steady oscillation may be respectively averaged as $\overline{P}_+$, $\overline{P}_-$, $\overline{A}_+$, and $\overline{A}_-$ for computation in the proposed identification algorithms. The oscillation period can thus be obtained as $\overline{P}_u = \overline{P}_+ + \overline{P}_-$. Accordingly, the process gain and response at the oscillation frequency can be computed, respectively, as

$$k_p = \frac{\int_{t_0}^{t_0+N\overline{P}_u} y(t)dt}{\int_{t_0}^{t_0+N\overline{P}_u} u(t)dt} \tag{4.2}$$

$$G(j\overline{\omega}_u) = \frac{\int_{t_0}^{t_0+N\overline{P}_u} y(t)e^{-j\overline{\omega}_u t}dt}{\int_{t_0}^{t_0+N\overline{P}_u} u(t)e^{-j\overline{\omega}_u t}dt} = \overline{A}_u e^{j\overline{\varphi}_u} \tag{4.3}$$

where $\overline{\omega}_u = 2\pi/\overline{P}_u$, N is the number of oscillation periods for averaging which may be taken in the range of $10 \sim 20$, and t_0 may be chosen as any relay switch point in steady oscillation. Note that the relay output, $u(t)$, remains as a constant for each half period, so it may be used for measurement of the oscillation period. When an unbiased relay feedback test is performed, N may be taken in the range of $5 \sim 10$, owing to that $\overline{P}_+ = \overline{P}_-$, $|\overline{A}_+| = |\overline{A}_-|$, and $\overline{P}_u = 2\overline{P}_+ = 2\overline{P}_-$.

Note that the above usage of the measured parameters is based on the statistical principle for eliminating random measurement errors, and therefore, is capable of identification robustness in the presence of low NSR (e.g., <10%).[23–26] To cope with measurement noises causing high NSR, a low-pass Butterworth filter is suggested to recover the corrupted limit cycle for measurement. It may be determined by specifying the filter order, nf, and the cutoff angular frequency, ω_c, i.e.,

$$\mathrm{Butter}(n_f, \omega_c) = \frac{b_1 + b_2 z^{-1} + b_3 z^{-2} + \cdots + b_{n_f+1} z^{-n_f}}{1 + a_2 z^{-1} + a_3 z^{-2} + \cdots + a_{n_f+1} z^{-n_f}} \tag{4.4}$$

where Butter(n_f, ω_c) denotes the filter function with two input parameters of n_f and ω_c. In view of that measurement noises are mainly of high-frequency, the guideline for choosing the cutoff angular frequency is given as

$$\omega_c \geq 5\omega_u = 10\pi/P_u \tag{4.5}$$

Thereby, only the signal components within the frequency band around ω_u can be passed through entirely. Note that the phase lag caused by the low-pass filter almost does not affect measurement of the oscillation period and the amplitude of the limit cycle, because the relay output has the similar phase lag under the filtered feedback.

Case studies

Here, five examples from the recent literature are used to illustrate the effectiveness and merits of the proposed identification algorithms. Examples 1–3 are given to demonstrate accuracy of the proposed algorithms for identification of the three types of SOPDT processes, overdamped, critically damped and underdamped. Measurement noises are also introduced in the three examples to illustrate robustness of the proposed identification algorithms. Examples 4 and 5 are performed to show the fitting effect of the proposed identification algorithms for higher order processes where model order mismatch exists as often encountered in practice. To assess the fitting error, the widely adopted fitting criterions of the maximal frequency response error, ERR, and the step response error, *err*, are used herein. For low-order controller design, the maximal frequency response error is usually defined as[19,20]

$$\mathrm{ERR} = \max_{\omega\in[0,\omega_c]} \left\{ \left| \frac{\hat{G}(j\omega) - G(j\omega)}{G(j\omega)} \right| \times 100\% \right\}$$

where ω_c is the cutoff angular frequency corresponding to $\angle G(j\omega_c) = -\pi$. Owing to that ω_u can be intuitively measured from a relay test and is slightly smaller than ω_c, it is hereby adopted to compute ERR for convenience.

The step response error is generally defined by the standard deviation for the transient response to a unity step change,[19,20] i.e.,

$$err = \frac{1}{N_s}\sum_{k=1}^{N_s}[\hat{y}(kT_s) - y(kT_s)]^2$$

where $\hat{y}(kT_s)$ and $y(kT_s)$ denotes respectively the model and process outputs, and N_sT_s is the transient response time or the settling time under a unity step change.

Example 1. Consider the overdamped second-order process widely studied in the literature[8–11]:

$$G = \frac{e^{-2s}}{(10s+1)(s+1)}$$

The enhanced ATV method[8] gave a SOPDT model, $G_m = 0.853e^{-2s}/(7.416s + 1)(1.15s + 1)$, by using two different relay tests with precise measurement of the process time delay. By using a single biased relay test, Ramakrishnan and Chidambaram[11] derived a SOPDT model, $G_m = 1.05e^{-1.814s}/(9.766s + 1)(1.271s + 1)$. Based on a biased ($u_+ = 1.3$ and $u_- = -0.7$) and an unbiased ($u_+ = -u_- = 1.0$) relay tests with $\varepsilon_+ = -\varepsilon_- = 0.2$ to avoid incorrect relay switches from measurement noises, respectively, the proposed Algorithm-O-A and Algorithm-O-B results in the process models listed in Table 2, together with the intermediate values for computation. It can be seen that high accuracy is obtained, corresponding to very small fitting errors.

Note that Ramakrishnan and Chidambaram[11] derived a SOPDT model, $G_m = 1.06e^{-2.04s}/(10.73s + 1)(0.92s + 1)$, on condition that a random measurement noise with zero mean and the standard deviation of 0.5% is added to the relay feedback channel. It can be verified that this measurement noise causes NSR = 2%. By using the averaging method for measurement of 10 oscillation periods in the time interval [60, 260](*s*), the proposed Algorithm-O-A results in the process model listed in Table 3, indicating good identification robustness. It should be noted that the similar results can also be obtained by the proposed Algorithm-O-B and thus are omitted.

To further demonstrate identification robustness against measurement noises, a random noise of $N(0, \sigma_N^2 = 0.055\%)$ is supposed to corrupt the process output measurement and relay feedback, causing NSR = 10%. It can be seen from Table 3 that the averaging method results in notable identification errors for the model parameters, which, however, is still acceptable for practice, as can be verified from the fitting errors. To enhance identification accuracy, a first-order Butterworth filter with the cutoff angular frequency $\omega_c = 3.5$(rad/s) according to the guideline given by (4.5) is used for the output measurement and relay feedback, leading to apparently improved identification robustness, as indicated by the resulting model shown in Table 3. Note that even for the case that a random noise causing NSR = 30% is added, using the proposed filter together with the averaging method for 10 oscillation periods, e.g., in the time interval [100, 320](*s*), is also capable of good identification robustness, as indicated by the resulting model and fitting errors listed in Table 3.

Example 2. Consider the critically damped second-order process studied by Thyagarajan and Yu[14]:

$$G = \frac{e^{-10s}}{(s+1)^2}$$

Thyagarajan and Yu[14] presented a rough estimation of the corresponding SOPDT model from a single unbiased relay test. Using the proposed Algorithm-C-A and Algorithm-C-B, the process models obtained from a single biased or unbiased relay test as in example 1 are respectively listed in Table 2, indicating that the proposed algorithms yield high accuracy for critically damped second-order processes. By performing the measurement noise tests as in example 1, the models obtained using Algorithm-C-A are listed in Table 3 along with the measured errors of the intermediate values for computation, demonstrating good identification robustness.

Example 3. Consider the underdamped second-order process studied by Panda and Yu[6]:

$$G = \frac{e^{-7s}}{s^2 + 0.4s + 1)}$$

Panda and Yu[6] derived a SOPDT model, $G_m = 1.05e^{-6.8902s}/(1.03s^2 + 0.41s + 1)$, from a single unbiased relay test. By performing a biased ($u_+ = 0.3$ and $u_- = -0.2$) and an unbiased ($u_+ = -u_- = 0.2$) relay tests with $\varepsilon_+ = -\varepsilon_- = 0.1$, respectively, the proposed Algorithm-U-A and Algorithm-U-B result in the SOPDT models listed in Table 2, indicating that high identification accuracy can thus be obtained. To demonstrate identification robustness, measurement noise tests are performed as in example 1, the resulting models from Algorithm-U-A are listed in Table 3, also indicating good identification robustness.

Example 4. Consider the high-order process studied in the literature[8,11]:

$$G = \frac{e^{-4s}}{(0.5s+1)^3}$$

The enhanced ATV method[8] gave a FOPDT model, $G_m = 1.0841e^{-4.04s}/(1.6362s + 1)$, and Ramakrishnan and Chidambaram[11] derived an overdamped SOPDT model, $G_m = 1.0046e^{-4.4239s}/(0.2286s + 1)(0.8839s + 1)$, from a single biased relay test. Based on the guidelines given for model structure selection in terms of the relay response shape, the proposed Algorithm-C-A is adopted to derive a SOPDT model from a single biased relay test as in example 1. The critically damped SOPDT model thus obtained is listed in Table 2. For comparison, the Nyquist plots of these models are shown in Figure 7. It can be seen that obviously improved fitting is captured by the proposed SOPDT model.

Example 5. Consider the high-order process studied in the literature[12,17]:

$$G = \frac{e^{-0.5s}}{(s+1)(s^2+s+1)}$$

Based on a single biased relay test, Wang et al.[17] gave a FOPDT model, $G_m = 1.00e^{-2.1s}/(1.152s + 1)$, which had shown apparently enhanced fitting effect in comparison with the ATV method,[2] and Kaya and Atherton[12] derived a critically damped SOPDT model, $G_m = 1.00e^{-1.633s}/(0.785s + 1)^2$. According to the characteristics of the relay response shape obtained from a single biased relay test as in example 1, the proposed Algorithm-U-A is chosen to derive a SOPDT model, resulting in an underdamped model listed in Table 2. For comparison, the Nyquist plots of these models are shown in Figure 8, which indicates again that obviously improved fitting is captured by the proposed SOPDT model, in particu-

Table 2. Identified Models for Five Processes from a Single Relay Feedback Test

		Limit Cycle						SOPDT Model Type			Fitting Error	
Process	Relay	P_+	P_-	A_+	A_-	A_u	φ_u	Overdamped	Critically damped	Underdamped	*err*	ERR
$\frac{e^{-2s}}{(10s+1)(s+1)}$	Biased	6.99	11.72	0.4222	−0.2953	0.2705	−2.2787	$\frac{1.0000e^{-1.9991s}}{(9.9921s+1)(1.0073s+1)}$			6.23×10^{-9}	0.17%
	Unbiased	8.73	8.73	0.3571	−0.3571	0.2519	−2.3667	$\frac{1.0122e^{-2.0037s}}{(10.1178s+1)(0.992s+1)}$			8.53×10^{-5}	1.22%
$\frac{e^{-10s}}{(s+1)^2}$	Biased	11.53	12.7	1.2998	−0.6999	0.937	−3.1019		$\frac{1.0000e^{-10s}}{(1.0001s+1)^2}$		2.5×10^{-10}	0.005%
	Unbiased	12.03	12.03	0.9998	−0.9998	0.9362	−3.1237		$\frac{1.0003e^{-9.9999s}}{(1.0027s+1)^2}$		1.54×10^{-7}	0.13%
$\frac{e^{-7s}}{s^2+0.4s+1}$	Biased	8.46	8.73	0.5823	−0.4728	1.1381	−2.7276		$\xi = 0.2001$, $\tau_p = 1.0001$	$\frac{1.0000e^{-7.004s}}{1.0004s^2+0.4009s+1}$	6.73×10^{-7}	0.19%
	Unbiased	8.66	8.66	0.4248	−0.4248	1.1359	−2.7084		$\xi = 0.2001$, $\tau_p = 1.0006$	$\frac{0.9999e^{-7.0044s}}{1.0012s^2+0.4004s+1}$	1.01×10^{-6}	0.18%
$\frac{e^{-4s}}{(0.5s+1)^3}$	Biased	5.24	5.96	−0.6989	1.2964	0.8926	−3.0672		$\frac{1.0000e^{-4.2771s}}{(0.6183s+1)^2}$		2.16×10^{-5}	0.36%
$\frac{e^{-0.5s}}{(s+1)(s^2+s+1)}$	Biased	2.71	3.53	1.0676	−0.7059	0.6996	−2.8818		$\xi = 0.719$, $\tau_p = 0.9871$	$\frac{1.0000e^{-1.3105s}}{0.9744s^2+1.4194s+1}$	7.12×10^{-4}	11.85%

Table 3. Denoising Effects for Identification Against Measurement Noises

NSR	Denoising	Example	% Error in the Intermediate Values				Identified Model	Fitting Error	
			A_+	A_-	A_u	φ_u		*err*	ERR
2%	Averaging	1	1.56	−2.07	−1.1	0.56	$\frac{0.9943e^{-1.9329s}}{(9.8346s+1)(1.098s+1)}$	1.9×10^{-5}	0.57%
		2	−8.9	4.89	−0.02	0.29	$\frac{1.0003e^{-10.0029s}}{(1.0009s+1)^2}$	1.54×10^{-7}	0.12%
		3	2.65	−2.47	0.01	−0.04	$\frac{1.0006e^{-7.0521s}}{0.9774s^2+0.3595s+1}$	1.53×10^{-4}	0.22%
10%	Averaging	1	−5.36	4.4	−9.64	−5.6	$\frac{1.0279e^{-2.5707s}}{(10.8686s+1)(0.3197s+1)}$	4.42×10^{-4}	3.27%
		2	−43.44	24.01	0.75	−2.93	$\frac{1.0025e^{-10.1809s}}{(1.0741s+1)^2}$	6.9×10^{-4}	8.29%
		3	12.28	−14.67	0.24	−0.94	$\frac{1.0025e^{-6.6759s}}{1.1618s^2+0.6823s+1}$	2.86×10^{-3}	0.63%
10%	Filtering	1	−3.56	4.6	3.97	1.7	$\frac{1.0012e^{-2.2686s}}{(10.0433s+1)(1.0216s+1)}$	4.16×10^{-5}	9.38%
		2	−3.81	2.14	0.02	0.15	$\frac{1.001e^{-10.2691s}}{(1.0359s+1)^2}$	5.08×10^{-4}	8.47%
		3	−0.02	−0.02	−1.54	−0.81	$\frac{1.0011e^{-7.375s}}{0.9296s^2+0.3659s+1}$	2.48×10^{-3}	9.46%
30%	Filtering	1	−3.8	7.96	3.2	−2.05	$\frac{1.0022e^{-2.2091s}}{(9.9832s+1)(1.0878s+1)}$	3.44×10^{-5}	9.27%
		2	−12.16	7.08	0.06	−0.01	$\frac{1.0041e^{-10.2287s}}{(1.05584s+1)^2}$	7.68×10^{-4}	8.4%
		3	1.93	−1.03	−1.47	−0.78	$\frac{1.0023e^{-7.4661s}}{0.8943s^2+0.2795s+1}$	3.87×10^{-3}	11.51%

lar for the referred low frequency range for controller design. Note that the proposed model response at (−0.676, −j0.18) corresponding to the oscillation frequency coincides precisely with that of the real process.

To demonstrate the achievable control performance in terms of the identified models, the standard internal model control structure (IMC)[27] is herein used. Following the IMC theory,[27] the IMC controller based on a perfect knowledge of the process should be designed as $Q_p = (s+1)(s^2+s+1)/(\lambda_p s+1)^3$, where λ_P is an adjustable control parameter, the IMC controller based on the proposed SOPDT model should be $Q_A = (0.9744s^2+1.4194s+1)/(\lambda_A s+1)^2$, the IMC

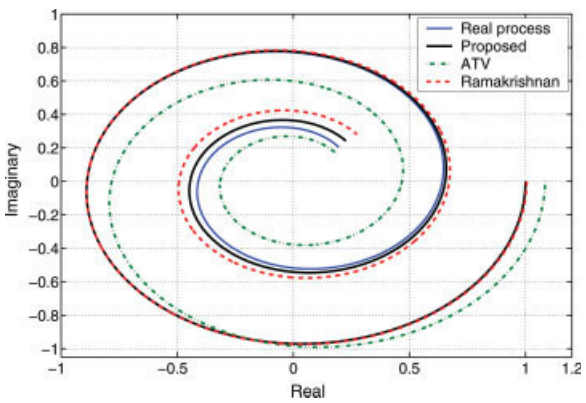

Figure 7. Nyquist fitting effect for example 4.

[Color figure can be viewed in the online issue, which is available at www.interscience.wiley.com.]

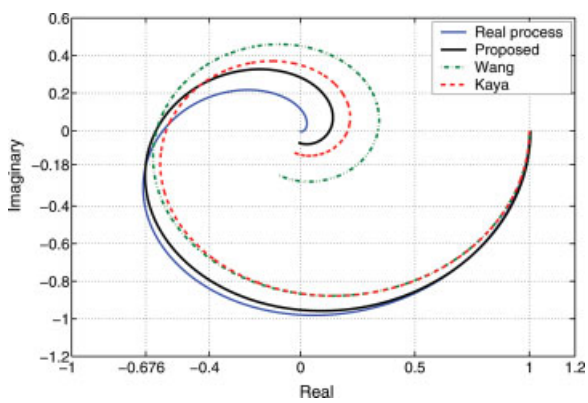

Figure 8. Nyquist fitting effect for example 5.

[Color figure can be viewed in the online issue, which is available at www.interscience.wiley.com.]

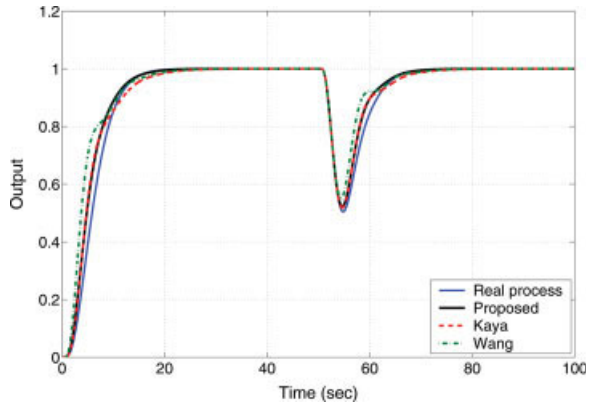

Figure 9. Nominal system response for example 5.

[Color figure can be viewed in the online issue, which is available at www.interscience.wiley.com.]

controller based on the SOPDT model of Kaya and Atherton[12] should be $Q_K = (0.785s + 1)^2/(\lambda_K s + 1)^2$, and the IMC controller based on the FOPDT model of Wang et al.[17] should be $Q_W = (1.152s+1)/(\lambda_W s + 1)$. By adding a unity step change to the set-point and then a step load disturbance with a magnitude of 0.5 to the process, and taking $\lambda_p = 2.0$, $\lambda_A = \lambda_K = 2.2$, and $\lambda_W = 3.0$ to obtain the same rising speed of the set-point response for comparison, the corresponding output responses are shown in Figure 9, respectively. It is seen that the proposed SOPDT model contributes to good control performance. Then, assume that the real process is perturbed due to some uncertainties, e.g., in the form of $G = e^{-2.5s}/(0.5s + 1)(s^2 + 0.5s + 1)$, the perturbed output responses shown in Figure 10 demonstrate that the proposed SOPDT model facilitates good control robustness.

Conclusions

A systematic on-line identification method has been proposed for obtaining a SOPDT process model from a single biased/unbiased relay feedback test. By classifying the relay response shapes of the three types of SOPDT model, overdamped, critically damped, and underdamped, guidelines have been established for model structure selection. For assessing process response under relay feedback test, exact relay response expressions of these low-order process models have been respectively derived based on the corresponding limit cycle analysis. Then the corresponding identification algorithms have been transparently developed by using the measurable parameters of these limit cycles. To ensure identification robustness in the presence of measurement noises, a statistical averaging method has been given for low noise level, e.g., NSR $< 10\%$, and a low-pass Butterworth filter is suggested to recover the corrupted limit cycle from measurement noises causing higher NSR. The applications to five examples studied in the recent literature have effectively demonstrated that the proposed identification algorithms are capable of good accuracy and robustness.

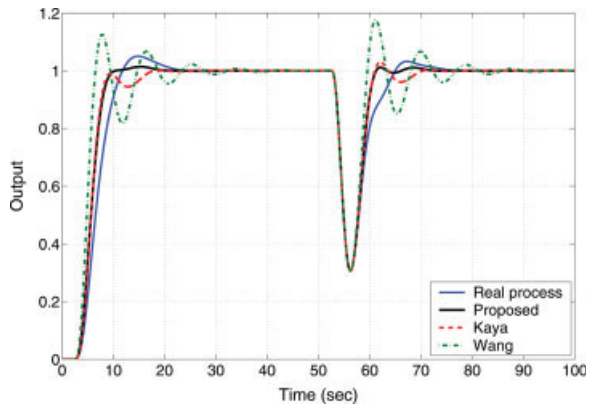

Figure 10. Perturbed system response for example 5.

[Color figure can be viewed in the online issue, which is available at www.interscience.wiley.com.]

Acknowledgments

This work is supported in part by the Hong Kong Research Grants Council under Project No. 612906.

Literature Cited

1. Åström KJ, Hägglund T. Automatic tuning of simple regulators with specification on phase angle and amplitude margins. *Automatica*. 1984;20:645–651.
2. Luyben WL. Derivation of transfer functions for highly nonlinear distillation columns. *Ind Eng Chem Res*. 1987;26:2490–2495.
3. Atherton DP. Relay Autotuning: an overview and alternative approach. *Ind Eng Chem Res*. 2006;45:4075–4080.
4. Hang CC, Åström KJ, Wang QG. Relay feedback auto-tuning of process controllers—a tutorial review. *J Process Control*. 2002;12:143–163.
5. Vivek S, Chidambaram M. Identification using single symmetrical relay feedback test. *Comput Chem Eng*. 2005;29:1625–1630.
6. Panda RC. Estimation of parameters of underdamped second order plus dead time processes using relay feedback. *Comput Chem Eng*. 2006;30:832–837.
7. Huang HP, Jeng JC, Luo KY. Auto-tune system using single-run relay feedback test and model-based controller design. *J Process Control*. 2005;15:713–727.
8. Li W, Eskinat E, Luyben WL. An improved autotune identification method. *Ind Eng Chem Res*. 1991;30:1530–1541.
9. Shen SH, Wu JS, Yu CC. Use of biased-relay feedback for system identification. *AIChE J*. 1996;42:1174–1180.
10. Srinivasan K, Chidambaram M. Modified relay feedback method for improved system identification. *Comput Chem Eng*. 2003;27:727–732.
11. Ramakrishnan V, Chidambaram M. Estimation of a SOPTD transfer function model using a single asymmetrical relay feedback test. *Comput Chem Eng*. 2003;27:1779–1784.
12. Kaya I, Atherton DP. Parameter estimation from relay autotuning with asymmetric limit cycle data. *J Process Control*. 2001;11:429–439.
13. Seborg DE, Edgar TF, Mellichamp DA. *Process Dynamic and Control*, 2nd ed. New Jersey: Wiley, 2004.
14. Thyagarajan T, Yu CC. Improved autotuning using the shape factor from relay feedback. *Ind Eng Chem Res*. 2003;42:4425–4440.
15. Panda RC, Yu CC. Shape factor of relay response curves and its use in autotuning. *J Process Control*. 2005;15:893–906.
16. Luyben WL. Getting more information from relay feedback tests. *Ind Eng Chem Res*. 2001;40:4391–4402.
17. Wang QG, Hang CC, Zou B. Low-order modelling from relay feedback. *Ind Eng Chem Res*. 1997;36:375–381.
18. Lin C, Wang QG, Lee TH. Relay feedback: a complete analysis for first-order systems. *Ind Eng Chem Res*. 2004;43:8400–8402.
19. Wang QG, Lee TH, Lin C. *Relay Feedback: Analysis, Identification and Control*. London: Springer-Verlag, 2003.
20. Yu CC. *Autotuning of PID Controllers: A Relay Feedback Approach*, 2nd ed. London: Springer-Verlag, 2006.
21. Tan KK, Lee TH, Wang QG. Enhanced automatic tuning procedures for process control of PI/PID Controllers. *AIChE J*. 1996;42:2555–2562.
22. Panda RC, Yu CC. Analytical expressions for relay feed back responses. *J Process Control*. 2003;13:489–501.

23. Tan KK, Ferdous R. Robustness assessment and control design using a relay feedback approach. *Ind Eng Chem Res*. 2006;45:4020–4027.
24. Sung SW, Lee J, Lee DH, Han JH, Park YS. Two-channel relay feedback method under static disturbances. *Ind Eng Chem Res*. 2006; 45:4071–4074.
25. Scali C, Marchetti G, Semino D. Relay with additional delay for identification and autotuning of completely unknown processes. *Ind Eng Chem Res*. 1999;38:1987–1997.
26. Liu T, Gao F. Alternative identification algorithms for obtaining a first-order stable/unstable process model from a single relay feedback test. *Ind Eng Chem Res*. 2007;47:1140–1149.
27. Morari M, Zafiriou E. *Robust Process Control*. Englewood Cliffs, NJ: Prentice Hall, 1989.

Appendix (I): Proof of Proposition 1

The initial step response of a critically damped SOPDT process arising from the relay output, $\Delta\mu-\mu_0$, can be derived as

$$y_0(t) = k_p(\Delta\mu - \mu_0)\left[1 - \left(1 + \frac{t-\theta}{t_p}\right)e^{-\frac{t-\theta}{\tau_p}}\right] \quad \text{(I.1)}$$

When it comes to the first relay switch point denoted by t_0 as shown in Figure 4a, the relay output changes to $\Delta\mu + \mu_0$, indicating that a step change of $2\mu_0$ is added to the process input. Using the linear superposition principle, the process output response can be derived as

$$y_1(t) = y_0(t+t_0) + 2k_p\mu_0 - 2k_p\mu_0\left(1 + \frac{t-\theta}{t_p}\right)e^{-\frac{t-\theta}{\tau_p}} \quad \text{(I.2)}$$

By using a time shift of $t_0 + \theta$, (I.2) can be rewritten as

$$y_1\big|_{\text{shift}}(t) = y_0(t+t_0+\theta) + 2k_p\mu_0 - 2k_p\mu_0\left(1 + \frac{t}{\tau_p}\right)e^{-\frac{t}{\tau_p}} \quad \text{(I.3)}$$

When it comes to the second relay switch point, the relay output changes to $\Delta\mu - \mu_0$, indicating that a step change of $-2\mu_0$ is added to the process input. Again using the linear superposition principle, the process output response can be derived as

$$y_2(t) = y_1(t+P_+) - 2k_p\mu_0 + 2k_p\mu_0\left(1 + \frac{t-\theta}{t_p}\right)e^{-\frac{t-\theta}{\tau_p}} \quad \text{(I.4)}$$

Using a time shift of $t_0 + \theta + P_+$, (I.4) can be rewritten as

$$y_2\big|_{\text{shift}}(t) = y_0(t+t_0+\theta+P_+) + 2k_p\mu_0(1-1) - 2k_p\mu_0 e^{-\frac{t}{\tau_p}} \left\{e^{-\frac{P_+}{\tau_p}} - 1 + \frac{1}{\tau_p}\left[t\left(e^{-\frac{P_+}{\tau_p}} - 1\right) + P_+ e^{-\frac{P_+}{\tau_p}}\right]\right\} \quad \text{(I.5)}$$

At the third relay switch point, the relay output changes again to $\Delta\mu + \mu_0$, indicating that a step change of $2\mu_0$ is once again added to the process input. The process output response with a time shift of $t_0 + \theta + P_u$ can be derived accordingly as

$$y_3\big|_{\text{shift}}(t) = y_0(t+t_0+\theta+P_u) + 2k_p\mu_0(1-1+1) - 2k_p\mu_0 e^{-\frac{t}{\tau_p}}\left\{e^{-\frac{P_u}{\tau_p}} - e^{-\frac{P_-}{\tau_p}} + 1 + \frac{1}{\tau_p}\left[t\left(e^{-\frac{P_u}{\tau_p}} - e^{-\frac{P_-}{\tau_p}} + 1\right) + P_u e^{-\frac{P_u}{\tau_p}} - P_- e^{-\frac{P_-}{\tau_p}}\right]\right\} \quad \text{(I.6)}$$

where $P_u = P_+ + P_-$.

The process output response following the fourth relay switch point is the result of four interlaced step changes respectively with a magnitude of $2\mu_0$. The process output response with a time shift of $t_0 + \theta + P_u + P_+$ can thus be derived as

$$y_4\big|_{\text{shift}}(t) = y_0(t+t_0+\theta+P_u+P_+) + 2k_p\mu_0(1-1+1-1) - 2k_p\mu_0 e^{-\frac{t}{\tau_p}}\left\{e^{-\frac{P_u+P_+}{\tau_p}} - e^{-\frac{P_u}{\tau_p}} + e^{-\frac{P_+}{\tau_p}} - 1 + \frac{1}{\tau_p}\left[t\left(e^{-\frac{P_u+P_+}{\tau_p}} - e^{-\frac{P_u}{\tau_p}} + e^{-\frac{P_+}{\tau_p}} - 1\right) + (P_u+P_+)e^{-\frac{P_u+P_+}{\tau_p}} - P_u e^{-\frac{P_u}{\tau_p}} + P_+ e^{-\frac{P_+}{\tau_p}}\right]\right\} \quad \text{(I.7)}$$

It can be summarized from (I.3–I.7) that

$$y_{2n+1}\big|_{\text{shift}}(t) = y_0(t+t_0+\theta+nP_u) + 2k_p\mu_0 - 2k_p\mu_0 e^{-\frac{t}{\tau_p}}\left[E_1 + \frac{(E_1 t + E_2)}{\tau_p}\right] \quad \text{(I.8)}$$

$$y_{2n+2}\big|_{\text{shift}}(t) = y_0(t+t_0+\theta+nP_u+P_+) - 2k_p\mu_0 e^{-\frac{t}{\tau_p}}\left[F_1 + \frac{(F_1 t + F_2)}{\tau_p}\right] \quad \text{(I.9)}$$

where $n = 0, 1, 2, \ldots$, and

$$E_1 = 1 + \sum_{k=1}^{n}\left(e^{-\frac{kP_u}{\tau_p}} - e^{-\frac{(k-1)P_u+P_-}{\tau_p}}\right) \quad \text{(I.10)}$$

$$E_2 = \sum_{k=1}^{n} kP_u e^{-\frac{kP_u}{\tau_p}} - \sum_{k=1}^{n}[(k-1)P_u + P_-]e^{-\frac{(k-1)P_u+P_-}{\tau_p}} \quad \text{(I.11)}$$

$$F_1 = \sum_{k=0}^{n}\left(e^{-\frac{kP_u+P_+}{\tau_p}} - e^{-\frac{kP_u}{\tau_p}}\right) \quad \text{(I.12)}$$

$$F_2 = \sum_{k=0}^{n}\left[\left(kP_u + P_+\right)e^{-\frac{kP_u+P_+}{\tau_p}} - kP_u e^{-\frac{kP_u}{\tau_p}}\right] \quad \text{(I.13)}$$

In view of that $0 < e^{-P_u/\tau_p} < 1$, it follows as $n \to \infty$ that

$$\sum_{k=0}^{n} e^{-\frac{kP_u}{\tau_p}} = \frac{1}{1 - e^{-\frac{P_u}{\tau_p}}} \quad \text{(I.14)}$$

Note that

$$\lim_{n\to\infty}\sum_{k=1}^{n} kP_u e^{-\frac{kP_u}{\tau_p}} = \lim_{n\to\infty} P_u\left(\sum_{k=1}^{n} e^{-\frac{kP_u}{\tau_p}} + \sum_{k=2}^{n} e^{-\frac{kP_u}{\tau_p}} + \ldots + \sum_{k=n-1}^{n} e^{-\frac{kP_u}{\tau_p}} + e^{-\frac{nP_u}{\tau_p}}\right) = \lim_{n\to\infty}\frac{P_u}{1 - e^{-\frac{P_u}{\tau_p}}}\left(e^{-\frac{P_u}{\tau_p}} + e^{-\frac{2P_u}{\tau_p}} + \ldots + e^{-\frac{(n-1)P_u}{\tau_p}} + e^{-\frac{nP_u}{\tau_p}}\right) = \frac{P_u e^{-\frac{P_u}{\tau_p}}}{\left(1 - e^{-\frac{P_u}{\tau_p}}\right)^2} \quad \text{(I.15)}$$

By substituting (I.14) and (I.15) into (I.10–I.13), we can obtain the simplified forms of E_1, E_2, F_1, and F_2, as shown in (1.4–1.7).

Note that $y_0(t + t_0 + \theta + nP_u) = y_0(t + t_0 + \theta + nP_u + P_+) = k_p(\Delta\mu - \mu_0)$ as $n \to \infty$. Hence, in the limit cycle, it follows that

$$y_+(t) = \lim_{n\to\infty} y_{2n+1}\big|_{\text{shift}}(t) = k_p(\Delta\mu + \mu_0) - 2k_p\mu_0 e^{-\frac{t}{\tau_p}}\left[E_1 + \frac{(E_1 t + E_2)}{\tau_p}\right], \quad t \in [0, P_+] \quad \text{(I.16)}$$

$$y_-(t) = \lim_{n\to\infty} y_{2n+2}\big|_{\text{shift}}(t) = k_p(\Delta\mu - \mu_0) - 2k_p\mu_0 e^{-\frac{t}{\tau_p}}[F_1 + \frac{(F_1 t + F_2)}{\tau_p}], \quad t \in [P_+, P_u] \qquad (I.17)$$

where $y_+(t)$ denotes the ascending process output response in a half period, P_+, due to a positive step change of the relay output, while $y_-(t)$ denotes the descending process output response in the other half period, P_-, due to a negative step change of the relay output.

It can be seen from the above derivation for (I.16) and (I.17) that the limit cycle can be definitely formed for a critically damped second-order process. It should be noted that before the process output response moves into a limit cycle, the time intervals between each relay switch points may not equal the corresponding half periods in the limit cycle. Nevertheless, we can equalize them as done in (I.4–I.7) to derive the exact expression of the limit cycle, in view of that the limit cycle does not include these initial response characteristics. In other words, the process response in steady oscillation has the same limit cycle with that of the corresponding ideal oscillation which has identical time intervals between the sequential relay switch points from beginning to end.

Note that E_2 shown in (1.5) can be reorganized as

$$E_2 = \frac{P_+ e^{-\frac{\rho u}{\tau_p}}(1 - e^{-\frac{p_-}{\tau_p}}) + p_- e^{-\frac{p_-}{\tau_p}}(e^{-\frac{p_+}{\tau_p}} - 1)}{(1 - e^{-\frac{\rho u}{\tau_p}})^2} \qquad (I.18)$$

Let

$$g(x) = \frac{1 - e^{-\frac{x}{\tau_p}}}{x}, \quad x \in (0, \infty) \qquad (I.19)$$

It follows that

$$\frac{dg(x)}{dx} = \frac{(\frac{x}{\tau_p} + 1)e^{-\frac{x}{\tau_p}} - 1}{x^2} < 0$$

Thus, it follows that $g(P_+) > g(P_-)$ since $P_+ < P_- < P_u$. Accordingly, it can be concluded from (I.18) that $E_2 < 0$. In a similar way, we can conclude that $F_2 > 0$.

Appendix (II): Proof of Proposition 2

The initial step response of an overdamped SOPDT process arising from the relay output, $\Delta\mu - \mu_0$, can be derived as

$$y_0(t) = k_p(\Delta\mu - \mu_0)\left(1 - \frac{\tau_1}{\tau_1 - \tau_2} e^{-\frac{t-\theta}{\tau_1}} + \frac{\tau_2}{\tau_1 - \tau_2} e^{-\frac{t-\theta}{\tau_2}}\right) \qquad (II.1)$$

Following a similar analysis as in Appendix (I) from the initial process response arising from the relay output, $\Delta\mu - \mu_0$, to the fourth relay switch point, the time shifted process output response after each relay switch point can be derived respectively as

$$y_1\big|_{\text{shift}}(t) = y_0(t + t_0 + \theta) + 2k_p\mu_0 - 2k_p\mu_0\left(\frac{\tau_1}{\tau_1 - \tau_2} e^{-\frac{t}{\tau_1}} - \frac{\tau_2}{\tau_1 - \tau_2} e^{-\frac{t}{\tau_2}}\right) \qquad (II.2)$$

$$y_2\big|_{\text{shift}}(t) = y_0(t + t_0 + \theta + P_+) + 2k_p\mu_0(1 - 1) - 2k_p\mu_0 \times \left[\frac{\tau_1}{\tau_1 - \tau_2} e^{-\frac{t}{\tau_1}}\left(e^{-\frac{P_+}{\tau_1}} - 1\right) - \frac{\tau_2}{\tau_1 - \tau_2} e^{-\frac{t}{\tau_2}}\left(e^{-\frac{P_+}{\tau_2}} - 1\right)\right] \qquad (II.3)$$

$$y_3\big|_{\text{shift}}(t) = y_0(t + t_0 + \theta + P_u) + 2k_p\mu_0(1 - 1 + 1) - 2k_p\mu_0 \times \left[\frac{\tau_1}{\tau_1 - \tau_2} e^{-\frac{t}{\tau_1}}\left(e^{-\frac{P_u}{\tau_1}} - e^{-\frac{P_-}{\tau_1}} + 1\right) - \frac{\tau_2}{\tau_1 - \tau_2} \times e^{-\frac{t}{\tau_2}}\left(e^{-\frac{P_u}{\tau_2}} - e^{-\frac{P_-}{\tau_2}} + 1\right)\right] \qquad (II.4)$$

$$y_4\big|_{\text{shift}}(t) = y_0(t + t_0 + \theta + P_u + P_+) + 2k_p\mu_0(1 - 1 + 1 - 1) - 2k_p\mu_0\left[\frac{\tau_1}{\tau_1 - \tau_2} e^{-\frac{t}{\tau_1}}\left(e^{-\frac{P_u + P_+}{\tau_1}} - e^{-\frac{P_u}{\tau_1}} + e^{-\frac{P_+}{\tau_1}} - 1\right) - \frac{\tau_2}{\tau_1 - \tau_2} \times e^{-\frac{t}{\tau_2}}\left(e^{-\frac{P_u + P_+}{\tau_2}} - e^{-\frac{P_u}{\tau_2}} + e^{-\frac{P_+}{\tau_2}} - 1\right)\right] \qquad (II.5)$$

The general relay response can be therefore summarized as

$$y_{2n+1}\big|_{\text{shift}}(t) = y_0(t + t_0 + \theta + nP_u) + 2k_p\mu_0 - 2k_p\mu_0 \times \left(\frac{\tau_1 E_1}{\tau_1 - \tau_2} e^{-\frac{t}{\tau_1}} - \frac{\tau_2 E_2}{\tau_1 - \tau_2} e^{-\frac{t}{\tau_2}}\right) \qquad (II.6)$$

$$y_{2n+2}\big|_{\text{shift}}(t) = y_0(t + t_0 + \theta + nP_u + P_+) - 2k_p\mu_0 \times \left(\frac{\tau_1 F_1}{\tau_1 - \tau_2} e^{-\frac{t}{\tau_1}} - \frac{\tau_2 F_2}{\tau_1 - \tau_2} e^{-\frac{t}{\tau_2}}\right) \qquad (II.7)$$

where $n = 0, 1, 2, \ldots$, and

$$E_1 = 1 + \sum_{k=1}^{n}(e^{-\frac{kP_u}{\tau_1}} - e^{-\frac{(k-1)P_u + P_-}{\tau_1}}) \qquad (II.8)$$

$$E_2 = 1 + \sum_{k=1}^{n}(e^{-\frac{kP_u}{\tau_2}} - e^{-\frac{(k-1)P_u + P_-}{\tau_2}}) \qquad (II.9)$$

$$F_1 = \sum_{k=0}^{n}(e^{-\frac{kP_u + P_+}{\tau_1}} - e^{-\frac{kP_u}{\tau_1}}) \qquad (II.10)$$

$$F_2 = \sum_{k=0}^{n}(e^{-\frac{kP_u + P_+}{\tau_2}} - e^{-\frac{kP_u}{\tau_2}}) \qquad (II.11)$$

By substituting (I.14) into (II.8–II.11), we can obtain the simplified forms of E_1, E_2, F_1 and F_2, as shown in (2.4–2.7).

Note that $y_0(t + t_0 + \theta + nP_u) = y_0(t + t_0 + \theta + nP_u + P_+) = k_p(\Delta\mu - \mu_0)$ as $n \to \infty$. Hence, in the limit cycle, it follows that

$$y_+(t) = \lim_{n\to\infty} y_{2n+1}\big|_{\text{shift}}(t) = k_p(\Delta\mu + \mu_0) - 2k_p\mu_0 \times \left(\frac{\tau_1 E_1}{\tau_1 - \tau_2} e^{-\frac{t}{\tau_1}} - \frac{\tau_2 E_2}{\tau_1 - \tau_2} e^{-\frac{t}{\tau_2}}\right), \quad t \in [0, P_+] \qquad (II.12)$$

$$y_-(t) = \lim_{n\to\infty} y_{2n+2}\big|_{\text{shift}}(t) = k_p(\Delta\mu - \mu_0) - 2k_p\mu_0\left(\frac{\tau_1 F_1}{\tau_1 - \tau_2} e^{-\frac{t}{\tau_1}} - \frac{\tau_2 F_2}{\tau_1 - \tau_2} e^{-\frac{t}{\tau_2}}\right), \quad t \in (P_+, P_u] \qquad (II.13)$$

It can be derived from (II.12) and (II.13) that

$$\frac{dy_+(t)}{dt} = \frac{2k_p\mu_0}{\tau_1 - \tau_2}\left(E_1 e^{-\frac{t}{\tau_1}} - E_2 e^{-\frac{t}{\tau_2}}\right) \qquad (II.14)$$

$$\frac{dy_-(t)}{dt} = \frac{2k_p\mu_0}{\tau_1 - \tau_2}(F_1 e^{-\frac{t}{\tau_1}} - F_2 e^{-\frac{t}{\tau_2}}) \tag{II.15}$$

To see if (II.14) and (II.15) have any positive solution for the time variable, t, we define $z = x/P_-$, $a = P_-/P_u$, and

$$f(x) = \frac{1 - e^{-\frac{P_-}{x}}}{1 - e^{-\frac{P_u}{x}}}, \quad x \in (0, \infty) \tag{II.16}$$

It follows that

$$f(z) = \frac{1 - e^{-\frac{1}{z}}}{1 - e^{-\frac{1}{az}}} \tag{II.17}$$

$$\frac{df(z)}{dz} = \frac{e^{-\frac{a+1}{az}}(e^{\frac{1}{z}} - ae^{-\frac{1}{az}} + a - 1)}{az^2(1 - e^{-\frac{1}{az}})^2} \tag{II.18}$$

Let

$$g(z) = e^{\frac{1}{z}} - ae^{\frac{1}{az}} + a - 1 \tag{II.19}$$

It can be verified that

$$\frac{dg(z)}{dz} = \frac{1}{z^2}(e^{\frac{1}{az}} - e^{\frac{1}{z}}) > 0 \tag{II.20}$$

$$\lim_{z \to \infty} g(z) = 0 \tag{II.21}$$

Thus, it can be concluded that $g(z) < 0$ for $z \in (0,\infty)$ and correspondingly,

$$\frac{df(z)}{dz} < 0 \tag{II.22}$$

Hence, $f(z)$ decreases monotonously with respect to z and so does for $f(x)$ with respect to x. We can then conclude from $f(\tau_1) < f(\tau_2)$ that $E_2 > E_1 > 0$. Following a similar analysis, it can be concluded that $F_2 < F_1 < 0$.

Appendix (III): Proof of Proposition 3

The initial step response of an underdamped SOPDT process arising from the relay output, $\Delta\mu - \mu_0$, can be derived as

$$y_0(t) = k_p(\Delta\mu - \mu_0)\left[1 - \frac{1}{\eta}e^{-\frac{\xi(t-\theta)}{\tau_p}}\sin\left(\frac{\eta(t-\theta)}{\tau_p} + \phi\right)\right] \tag{III.1}$$

Following a similar analysis as in Appendix (I) from the initial process response arising from the relay output, $\Delta\mu - \mu_0$, to the fourth relay switch point, the time shifted process output response after each relay switch point can be derived respectively as

$$y_1\big|_{\text{shift}}(t) = y_0(t + t_0 + \theta) + 2k_p\mu_0 - \frac{2k_p\mu_0}{\eta}e^{-\frac{\xi t}{\tau_p}}\sin\left(\frac{\eta t}{\tau_p} + \phi\right) \tag{III.2}$$

$$y_2\big|_{\text{shift}}(t) = y_0(t + t_0 + \theta + P_+) + 2k_p\mu_0(1 - 1) - \frac{2k_p\mu_0}{\eta} \times e^{-\frac{\xi t}{\tau_p}}\left[e^{-\frac{P_+\xi}{\tau_p}}\sin\left(\frac{\eta(t+P_+)}{\tau_p} + \phi\right) - \sin\left(\frac{\eta t}{\tau_p} + \phi\right)\right] \tag{III.3}$$

$$y_3\big|_{\text{shift}}(t) = y_0(t + t_0 + \theta + P_u) + 2k_p\mu_0(1 - 1 + 1) - \frac{2k_p\mu_0}{\eta}e^{-\frac{\xi t}{\tau_p}}\left[e^{-\frac{P_u\xi}{\tau_p}}\sin\left(\frac{\eta(t+P_u)}{\tau_p} + \phi\right) - e^{-\frac{P_-\xi}{\tau_p}} \times \sin\left(\frac{\eta(t+P_-)}{\tau_p} + \phi\right) + \sin\left(\frac{\eta t}{\tau_p} + \phi\right)\right] \tag{III.4}$$

$$y_4\big|_{\text{shift}}(t) = y_0(t + t_0 + \theta + P_u + P_+) + 2k_p\mu_0(1 - 1 + 1 - 1) - \frac{2k_p\mu_0}{\eta}e^{\frac{-\xi t}{\tau_p}}\left[e^{\frac{-(P_u+P_+)\xi}{\tau_p}}\sin\left(\frac{\eta(t+P_u+P_+)}{\tau_p} + \phi\right) - e^{-\frac{P_u\xi}{\tau_p}}\sin \times \left(\frac{\eta(t+P_u)}{\tau_p} + \phi\right) + e^{-\frac{P+\xi}{\tau_p}}\sin\left(\frac{\eta(t+P_+)}{\tau_p} + \phi\right) - \sin\left(\frac{\eta t}{\tau_p} + \phi\right)\right] \tag{III.5}$$

The general relay response can be therefore summarized as

$$y_{2n+1}\big|_{\text{shift}}(t) = y_0(t + t_0 + \theta + nP_u) + 2k_p\mu_0 - \frac{2k_p\mu_0 E}{\eta}e^{-\frac{\xi t}{\tau_p}} \tag{III.6}$$

$$y_{2n+2}\big|_{\text{shift}}(t) = y_0(t + t_0 + \theta + nP_u + P_+) - \frac{2k_p\mu_0 F}{\eta}e^{-\frac{\xi t}{\tau_p}} \tag{III.7}$$

where $n = 0, 1, 2, \ldots$, and

$$E = \sin\left(\frac{\eta t}{\tau_p} + \phi\right) + \sum_{k=1}^{n} e^{-\frac{kP_u\xi}{\tau_p}}\sin\left(\frac{\eta(t + kP_u)}{\tau_p} + \phi\right) - \sum_{k=1}^{n} e^{-\frac{[(k-1)P_u + P_-]\xi}{\tau_p}}\sin\left(\frac{\eta[t + (k-1)P_u + P_-]}{\tau_p} + \phi\right) \tag{III.18}$$

$$F = \sum_{k=0}^{n}\left[e^{-\frac{(kP_u+P_+)\xi}{\tau_p}}\sin\left(\frac{\eta(t + kP_u + P_+)}{\tau_p} + \phi\right) - e^{-\frac{kP_u\xi}{\tau_p}}\sin\left(\frac{\eta(t + kP_u)}{\tau_p} + \phi\right)\right] \tag{III.9}$$

Using the Euler formula, it follows that

$$\sum_{k=1}^{n} e^{-\frac{kP_u\xi}{\tau_p}}\sin\left(\frac{\eta(t + kP_u)}{\tau_p} + \phi\right) = \sum_{k=1}^{n} e^{-\frac{kP_u\xi}{\tau_p}} \cdot \frac{e^{j[\frac{\eta(t+kP_u)}{\tau_p} + \phi]} - e^{-j[\frac{\eta(t+kP_u)}{\tau_p} + \phi]}}{2j}$$

Then, using the convergent property shown in (I.14), we can obtain

$$\begin{aligned}
&\sum_{k=1}^{n} e^{-\frac{kP_u\xi}{\tau_p}}\sin\left(\frac{\eta(t + kP_u)}{\tau_p} + \phi\right) \\
&= \frac{e^{j(\frac{\eta t}{\tau_p} + \phi)}}{2j}\sum_{k=1}^{n} e^{-\frac{kP_u(\xi - j\eta)}{\tau_p}} - \frac{e^{-j(\frac{\eta t}{\tau_p} + \phi)}}{2j}\sum_{k=1}^{n} e^{-\frac{kP_u(\xi + j\eta)}{\tau_p}} \\
&= \frac{e^{j(\frac{\eta t}{\tau_p} + \phi)}}{2j} \cdot \frac{e^{-\frac{P_u(\xi - j\eta)}{\tau_p}}}{1 - e^{-\frac{P_u(\xi - j\eta)}{\tau_p}}} - \frac{e^{-j(\frac{\eta t}{\tau_p} + \phi)}}{2j} \cdot \frac{e^{-\frac{P_u(\xi + j\eta)}{\tau_p}}}{1 - e^{-\frac{P_u(\xi + j\eta)}{\tau_p}}} \\
&= -\sin\left(\frac{\eta t}{\tau_p} + \phi\right) + \frac{\sin(\frac{\eta t}{\tau_p} + \phi) - e^{-\frac{P_u\xi}{\tau_p}}\sin(\frac{\eta(t - P_u)}{\tau_p} + \phi)}{1 - 2e^{-\frac{P_u\xi}{\tau_p}}\cos\frac{\eta P_u}{\tau_p} + e^{-\frac{2P_u\xi}{\tau_p}}}
\end{aligned} \tag{III.10}$$

Similarly, it can be derived that

$$\sum_{k=0}^{n} e^{-\frac{(kP_u+P_-)\xi}{\tau_p}} \sin\left(\frac{\eta(t+kP_u+P_-)}{\tau_p}+\phi\right) = \frac{e^{-\frac{P_-\xi}{\tau_p}}[\sin(\frac{\eta(t+P_-)}{\tau_p}+\phi) - e^{-\frac{P_u\xi}{\tau_p}}\sin(\frac{\eta(t-P_+)}{\tau_p}+\phi)]}{1-2e^{-\frac{P_u\xi}{\tau_p}}\cos\frac{\eta P_u}{\tau_p}+e^{-\frac{2P_u\xi}{\tau_p}}} \quad \text{(III.11)}$$

Substituting (III.10) and (III.11) into (III.8) yields

$$E = \frac{\sin(\frac{\eta t}{\tau_p}+\phi) - e^{-\frac{P_u\xi}{\tau_p}}\sin(\frac{\eta(t-P_u)}{\tau_p}+\phi) - e^{-\frac{P_-\xi}{\tau_p}}[\sin(\frac{\eta(t+P_-)}{\tau_p}+\phi) - e^{-\frac{P_u\xi}{\tau_p}}\sin(\frac{\eta(t-P_+)}{\tau_p}+\phi)]}{1-2e^{-\frac{P_u\xi}{\tau_p}}\cos\frac{\eta P_u}{\tau_p}+e^{-\frac{2P_u\xi}{\tau_p}}} = \frac{\rho_1\sin(\frac{\eta t}{\tau_p}+\psi_1)}{\gamma} \quad \text{(III.12)}$$

where $\rho_1 = \sqrt{U_1^2+V_1^2}$, $\psi_1 = \tan^{-1}(V_1/U_1)$, and

$$\gamma = 1-2e^{-\frac{P_u\xi}{\tau_p}}\cos\frac{\eta P_u}{\tau_p}+e^{-\frac{2P_u\xi}{\tau_p}} \quad \text{(III.13)}$$

$$U_1 = \cos\phi - e^{-\frac{P_u\xi}{\tau_p}}\cos\left(\phi-\frac{\eta P_u}{\tau_p}\right) - e^{-\frac{P_-\xi}{\tau_p}}\left[\cos\left(\phi+\frac{\eta P_-}{\tau_p}\right) - e^{-\frac{P_u\xi}{\tau_p}}\cos(\phi-\frac{\eta P_+}{\tau_p})\right] \quad \text{(III.14)}$$

$$V_1 = \sin\phi - e^{-\frac{P_u\xi}{\tau_p}}\sin\left(\phi-\frac{\eta P_u}{\tau_p}\right) - e^{-\frac{P_-\xi}{\tau_p}}\left[\sin\left(\phi+\frac{\eta P_-}{\tau_p}\right) - e^{-\frac{P_u\xi}{\tau_p}}\sin(\phi-\frac{\eta P_+}{\tau_p})\right] \quad \text{(III.15)}$$

Following a similar derivation, we can obtain

$$F = -\frac{\rho_2\sin(\frac{\eta t}{\tau_p}+\psi_2)}{\gamma} \quad \text{(III.16)}$$

where $\rho_2 = \sqrt{U_2^2+V_2^2}$, $\psi_2 = \tan^{-1}(V_2/U_2)$, and

$$U_2 = \cos\phi - e^{-\frac{P_u\xi}{\tau_p}}\cos\left(\phi-\frac{\eta P_u}{\tau_p}\right) - e^{-\frac{P_+\xi}{\tau_p}}\left[\cos\left(\phi+\frac{\eta P_+}{\tau_p}\right) - e^{-\frac{P_u\xi}{\tau_p}}\cos\left(\phi-\frac{\eta P_-}{\tau_p}\right)\right] \quad \text{(III.17)}$$

$$V_2 = \sin\phi - e^{-\frac{P_u\xi}{\tau_p}}\sin\left(\phi-\frac{\eta P_u}{\tau_p}\right) - e^{-\frac{P_+\xi}{\tau_p}}\left[\sin\left(\phi+\frac{\eta P_+}{\tau_p}\right) - e^{-\frac{P_u\xi}{\tau_p}}\sin\left(\phi-\frac{\eta P_-}{\tau_p}\right)\right] \quad \text{(III.18)}$$

Note that $y_0(t + t_0 + \theta + nP_u) = y_0(t + t_0 + \theta + nP_u + P_+) = k_p(\Delta\mu - \mu_0)$ as $n \to \infty$. Hence, in the limit cycle, it follows that

$$y_+(t) = \lim_{n\to\infty} y_{2n+1}\big|_{\text{shift}}(t) = k_p(\Delta\mu+\mu_0) - \frac{2k_p\mu_0 E}{\eta}e^{-\frac{\xi t}{\tau_p}}, t\in[0,P_+] \quad \text{(III.19)}$$

$$y_-(t) = y_{2n+2}\big|_{\text{shift}}(t) = k_p(\Delta\mu-\mu_0) - \frac{2k_p\mu_0 F}{\eta}e^{-\frac{\xi t}{\tau_p}}, \quad t\in(P_+,P_u] \quad \text{(III.20)}$$

Manuscript received May 14, 2007, and revision received Feb. 3, 2008.